Available online at www.sciencedirect.com
SCIENCE DIRECT®

Fluid Dynamics Research 38 (2006) 174–210

FLUID DYNAMICS RESEARCH

Modelling turbulent separated flow in the context of aerodynamic applications

M.A. Leschziner*

Department of Aeronautics, Imperial College London, South Kensington Campus, London SW7 2AZ, UK

Received 15 June 2004; received in revised form 23 August 2004; accepted 2 November 2004

Communicated by F. Hamba

Abstract

In contrast to rapid advances in computing, numerical methods and visualisation, the predictive capabilities of statistical models of turbulence are limited and improve only slowly, despite much intensive research in the recent past. The intuitive nature of turbulence modelling, its strong reliance on calibration and validation, the extreme sensitivity of model performance to seemingly minor variations in modelling details and flow conditions, and the fact that the non-local dynamics of turbulence are not well captured by single-point closure, all conspire to make turbulence modelling an especially demanding component of CFD, but one that is crucially important for the correct prediction of complex flows. This applies in particular to separation from streamlined bodies, which is, from a computational point of view, the most challenging flow feature in aeronautical CFD.

This paper reviews some aspects of the foundation and application of turbulence models to flows that relate to aeronautical practice, with particular emphasis being placed on turbulence-transport models at a closure level higher than that based on the Boussinesq-viscosity hypothesis. Following a review of basic modelling issues, including aspects of linear-eddy-viscosity two-equation modelling, some recent experience and current work on predicting separation from continuous surfaces with non-linear eddy-viscosity models and second-moment closure are reported. The predictive performance of several anisotropy-resolving models is illustrated by reference to computational solutions for a number of flows, both two- and three-dimensional, some compressible and others incompressible.

Keywords: Aerodynamic separated flow; Turbulence modelling; Reynolds-stress models; Non-linear eddy-viscosity models; Curved surfaces; Computational fluid dynamics

* Tel.: +44 20 7594 5061; fax: +44 20 7584 8120.
E-mail address: m.leschziner@imperial.ac.uk.

0169-5983/$30.00
doi:10.1016/j.fluiddyn.2004.11.004

1. Introduction

Most aerodynamic flows are associated with fast-moving, slender, streamlined bodies. Such flows are characterised by low curvature, large irrotational (inviscid) regions, in which the motion is dictated by a balance between convection and pressure gradients, and relatively thin rotational (sheared) layers. Turbulence is usually only important in the highly sheared parts—the boundary layers on the surface of the body and the wakes that combine the boundary layers following their separation from trailing edges. Any large-scale vortices shed from wing tips or swept leading edges are essentially non-turbulent, except after they 'burst' and perhaps within their cores, prior to bursting, which are formed by turbulent boundary-layer fluid. While the fundamental turbulence mechanisms at play might be (indeed, *are*) complex even in these attached flows, the aeronautical engineer is usually only interested in a few global manifestations of turbulence: the skin friction, the displacement thickness of the boundary layer and its effect on the outer irrotational flow, and the momentum defect in the wake. These quantities are essentially dictated by a single statistical turbulence variable—the shear stress in the (local) streamwise direction. Although the determination of this stress is a non-trivial task, the focus on that single quantity, and the fact that the state of turbulence changes only slowly in the flow direction, allows highly simplified modelling approaches to be adopted, which side-step much of the fundamental physics and lean heavily on empirical correlation and calibration. Herein lies the reason for the prevalence and persistence of some especially simple turbulence models in aeronautical practice—models that reduce the turbulence-closure problem to the determination of a scalar *eddy viscosity* from an algebraic relationship or with the aid of a simple differential equation that takes into account the transport of a representative turbulence parameter.

Notwithstanding the above general categorisation, there are many aeronautical applications in which turbulence plays a much more influential role than in thin shear flows, and which require refined modelling techniques to provide an acceptably realistic predictive description. Many of these flows occur in off-design operational conditions and when the boundaries of the aerodynamic performance envelope are approached or, indeed, breached. In many cases, separation and recirculation are the key features that require resolution, but there are also non-separated flows in which turbulence is of major importance. Specific examples are:

- shock-induced boundary-layer thickening and separation on transonic wings, afterbodies, concave ramps and ahead of fins in supersonic flight;
- high-lift and stalled aerofoils—especially multi-element configurations;
- wing–body/fin-body junctions, which provoke strong horseshoe vortices and can include separation in the junction;
- vortical separation from streamlined bodies (e.g. fuselage) at high incidence;
- VSTOL flight with vectored jets;
- flow-control applications with vortex generators, such as fins and jets (both continuous and pulsed);
- dynamic stall in pitching and oscillating aerofoils; and
- exhaust jets, especially under-expanded supersonic jets featuring shock cells, with particular emphasis on spreading rate and infra-red visibility.

With the last example excluded, the major practical importance of turbulence arises from the fact that the sheared turbulent regions are sufficiently thick to cause appreciable changes to the irrotational flow around the load-bearing surfaces. In fact, in VSTOL applications, the highly turbulent impinging jets, the ensuing ground vortex and short-circuiting associated with hot-gas reingestion are the features of primary concern to the operational performance and safety of the aircraft. In the case of transonic and high-lift wings, the shock or adverse pressure gradient acting on the suction-side boundary layers lead to strong fluid deceleration, rapid boundary-layer thickening and possibly separation, with consequent dramatic loss of lift and increase in drag. The key process in wing/body-junction and vortex-generator flows is the creation of a recirculation zone upstream of the wing or vortex generator and the formation of a horseshoe vortex within which the transverse circulation redistributes streamwise momentum, thus inhibiting separation in the junction or downstream of the vortex generator.

The modelling challenges posed by the types of flow considered above are rooted in the complexity of the strain field and the high rates of change to which the flow as well as the turbulence fields are subjected. If attention is initially restricted to statistically steady, two-dimensional conditions, the complex flow features of primary concern are the strong streamwise straining provoked by the adverse pressure gradient (or shock), separation, reattachment and post-reattachment recovery. All are affected by the details of the turbulence structure, not simply by a single shear stress. The response of the decelerating boundary layer to the adverse pressure gradient, and hence the location of separation, is dictated by the turbulent shear stress ($\rho\overline{uv}$) as well as the normal stresses ($\rho\overline{u^2}$, $\rho\overline{v^2}$). The importance of the normal stresses is due to two interactions: first, the normal stresses are dynamically active (i.e., unlike in thin shear flow, gradients of the normal stresses contribute to the momentum balance); second, the shear stress is sensitive to normal straining and streamline curvature, and, as will be shown later, this linkage occurs via the normal stresses, which are themselves sensitive to streamwise, shear and curvature-related straining. Near a wall, turbulence is highly anisotropic, with $\overline{v^2} \ll \overline{u^2}$. This anisotropy, induced by a combination of different production rates for the normal stresses and the kinematic blocking effect of the wall, needs to be correctly captured if the shear stress is to be evaluated accurately. As the flow approaches separation, the behaviour of the near-wall layer departs drastically from any universal law of the wall, and its detailed structure must be resolved, including that of the semi-viscous sublayer in which viscosity affects turbulence. Similar comments apply to recirculation and reattachment regions. Thus, here too, the turbulent normal stresses are dynamically active, and the turbulence is sensitive to streamline curvature. A further complication in relation to reattachment is that the turbulent state in this region depends sensitively on the evolution of turbulence in the separated shear layer about to reattach. Finally, the near-wall layer in the recovery region combines the reattached shear layer and a new boundary layer emanating from the reattachment point. This poses the problem of how to deal with component flows containing very different scales, reflecting the different history of these components.

Much of the above discussion also applies to three-dimensional flows, but a number of additional complications require consideration. Many three-dimensional flows feature skewed boundary layers in which the direction of the velocity vector changes rapidly as the wall is approached. Coupled with this ‘rotation’ are rapid variations in the shear–stress components associated with the shear strains formed with the wall-parallel velocity components (however they are resolved within the chosen computational coordinate system) and the wall-normal coordinate. Hence, even in fully-attached conditions, and even if the influence of the normal turbulent stresses may be ignored, the task is now one of devising a turbulence closure capable of returning *two* shear–stress components and their interaction with skewness and curvature. When, in addition, closed or open separation occurs—say, as a result of two boundary layers ‘colliding’ obliquely in the leeward side of a relatively thick curved body, a boundary layer interacting with a fin or wing or two interacting wall jets associated with twin-jet ground impingement—streamwise vortices are generated, the size of which can be substantially larger than the thickness of the boundary layers prior to their interaction. In such circumstances, the multi-facetted coupling among all stresses and strain components, as well as the interaction between turbulence and the curvature associated with the transverse circulation in the vortex, become influential.

Unsteadiness introduces a fundamental and profound uncertainty into the RANS framework. Reynolds-averaging, whether ensemble- or time-based, presupposes that the flow is statistically steady. At the very least, the time-scale associated with the organised unsteady motion must be substantially larger than the time-scale of the turbulent motion—or, in other words: the two time-scales must be well separated. This condition may be satisfied, say, in low-frequency dynamic stall, but perhaps not in flutter or buffet. From a purely formal point of view, phase-averaging offers a rigorously valid route to deriving a statistical framework for unsteady flow. However, in practice, closure of the (phase-averaged) correlations is identical or very similar to that adopted for the conventionally-averaged correlations, and this inevitably leads to models which are formally identical to their steady counterparts.

Strictly, the only fundamentally secure approach to unsteadiness is via Direct Numerical Simulation (DNS) which resolves the entire spectrum of turbulent motions in all details. However, at Reynolds numbers pertinent to aerodynamic practice, the resource implications even of Large Eddy Simulations (LES) is prohibitive. A decisive element in the resource equation is the fact that most turbulent aerodynamic flows occur close to walls and are therefore strongly affected by viscous effects. However, near a wall, the 'large', dynamically influential turbulent scales are small, so that very dense meshes are required for a reasonable resolution of the flow. To give an example, one conclusion emerging from the recent EU project LESFOIL (Davidson et al., 2003), which investigated LES for high-lift aerofoils, is that the simulation of the marginally separated, transitional flow around a single-element, high-lift aerofoil at $Re = 2 \times 10^6$ (based on chord) would require an order of 100 million nodes for a spanwise extent of only 10% of chord. These resources are dramatically beyond what is economically tolerable in practice.

On the assumption that conventional turbulence models may be applied to (a restricted range of) unsteady flows, the level of closure may have important implications to predictive accuracy. Unsteadiness increases the rate of change of all flow quantities and results, in particular, in a phase lag between the mean motion and the turbulence quantities. A relevant parameter to consider is the ratio of the time scales of the mean motion $\Omega k/\varepsilon$, where k is the turbulence energy, ε is its rate of dissipation and Ω is the frequency of the mean motion. As the boundary layer is traversed towards the wall, this ratio declines rapidly, given a fixed frequency of mean-flow oscillation. The implication is that the turbulence structure close to the wall will adjust rapidly to the external oscillation, so that a quasi-steady turbulence closure would be expected to be adequate. However, towards the outer part of the boundary layer, the turbulence field will not respond quickly to the oscillation, and the turbulent stresses would tend to 'freeze', with consequent phase shift between the mean motion and the turbulence field. To take this into account, a turbulence model needs to account for stress transport. Hence, unsteady flows can, in general, be expected to benefit from second-moment closure, which entails a reduced level of reliance on equilibrium assumptions.

The present paper reviews aspects of modelling separated flows that are relevant to aerodynamic applications, with emphasis placed on anisotropy-resolving closures—that is, closures at the level higher than linear eddy-viscosity, two-equation models. The paper starts with a broad (although far from comprehensive) review of model formulations, within the range of categories mentioned above, which are frequently used in aerodynamics. This is followed by a discussion of experience reported in the literature in relation to the application of these models in a variety of aeronautical applications in which turbulence is highly influential, especially in flows featuring separation. Finally, a selection of results arising from studies by the writer with anisotropy-resolving models are presented and discussed, in order to provide a foundation and justification for some broad conclusions.

2. Turbulence modelling

2.1. Categories considered

There are three principal classes of models currently used in computations of practically relevant aerodynamic flows:

- linear eddy-viscosity models (LEVM), either algebraic or involving differential equations for one scalar turbulence quantity or two;
- non-linear eddy-viscosity models (NLEVM);
- Reynolds-stress models (RSM).

Some models do not fall neatly into any one of the above categories, straddling two categories or containing elements from more than one category. Thus,

- explicit algebraic Reynolds-stress models (EARSM) combine elements of NLEVM and RSM;
- the "V2F" model of Durbin (1995) (see also Parneix et al., 1998) is essentially a LEVM, but incorporates a simplified transport equation for the normal stress perpendicular to streamlines (or the wall), which serves as the turbulent-velocity scale in the eddy viscosity, in preference to the turbulence energy.

Other model types exist, but have not been used to any significant extent for practical computations. These include:

- the "Structure-Based Model" of Kassinos et al. (2000);
- various model proposals derived from two-point-correlation functions (e.g. Cambon and Scott, 1999).
- Multi-scale models, which are based on a partitioning of the turbulence-energy spectrum, each partition associated with a different size range of eddies (e.g. Schiestel, 1987; Wilcox, 1988a).

Within any one of the above major categories, there are dozens of variants, and the LEVM category, being the simplest, contains several sub-categories—based on algebraic, one-(differential)-equation and two-equation formulations—and is especially heavily populated with model variations, many differing from other forms by the inclusion of minor (though sometimes very influential) 'correction terms', realisability constraints or different functional forms of model coefficient, or even through slight differences in the numerical values of model constants. To a considerable degree, this proliferation reflects a trend to adopt or adhere to simple (too simple) turbulence models for the modelling task at hand and then to add 'patches' so as to 'cure' specific ills for specific sets of conditions. Other not unimportant contributory factors are insufficiently careful and excessively narrow validation, yielding misleading statements on the predictive capabilities of existing models, and the fact that publishing a 'new' model, rather than quantifying the capabilities of an existing model, is not only easier, but also gives greater prominence to the originator whose name is customarily attached to the model.

2.2. Linear eddy-viscosity models (LEVMs)

LEVM are based on the linear stress–strain relationship,

$$-\rho\overline{u_i u_j} = \mu_t \left(\frac{\partial U_i}{\partial x_j} + \frac{\partial U_j}{\partial x_i} - \frac{2}{3}\frac{\partial U_k}{\partial x_k}\delta_{ij} \right) - \frac{2}{3}\rho k \delta_{ij}. \tag{1}$$

Such models display a number of important defects, almost regardless of how μ_t is determined, which are especially pertinent to and influential in separated flow:

- they do not resolve normal-stress anisotropy;
- they do not account for transport of stresses, but link rigidly the stresses to the strain;
- they over-estimate the stresses at high strain rates;
- they do not respond correctly to curvature strain, normal straining and rotation (though ad hoc patches help in some circumstances);
- they seriously misrepresent, when used in conjunction with eddy-diffusivity/gradient-diffusion approximations, the heat fluxes, except for the flux component normal to simple shear layers with a dominant cross-layer temperature gradient.

Despite the above limitations, LEVM have been by far the most popular group of models in aeronautical CFD. One reason is that most aerodynamic flows involve rather thin, slowly evolving shear layers, in which the shear stress (often only one component) is the only dynamically active stress. Another, possibly even more important issue relating to the often extremely complex geometry and meshing problems, is the simplicity and economy of these models.

Algebraic models, now regarded as outdated, are mostly based on the mixing-length concept and are inappropriate for separated flows—although still happily used in aeronautical practice, even in the presence of separation, albeit with ad hoc corrections. All presume local turbulence equilibrium $-\overline{uv}(\partial U/\partial y) = \varepsilon$ (applicable to thin-shear flow), implying that the turbulence time scale (k/ε) is a fixed factor of the mean-flow time scale, via $\frac{k}{\varepsilon}(\partial U/\partial y) \approx 3.3$.

One-equation models take departures from local equilibrium into account, but only to a very limited extent. They require, either directly or indirectly, a prescription of the length scale or a related constraint which is tied to the equilibrium concept. This requirement is nearly as severe a limitation as that applicable to algebraic models, and one-equation models do not, therefore, generally display decisively superior predictive characteristics in wall flows departing substantially from equilibrium, unless specifically crafted by highly targeted calibration (e.g. via forcing functions) for such conditions. One such “highly crafted” model is that of Spalart and Allmaras (1992). Its basic high-*Re* form is

$$\frac{\partial v_t}{\partial t} + \frac{\partial U_j v_t}{\partial x_j} = C_1 v_t S + \frac{1}{\sigma}\frac{\partial}{\partial x_j}\left(v_t \frac{\partial v_t}{\partial x_j} \right) + \frac{C_2}{\sigma}\left(\frac{\partial v_t}{\partial x_j} \right)^2 - C_w f_w \left(\frac{v_t}{d} \right)^2. \tag{2}$$

It relies heavily on calibration by reference to a wide range of experimental data, including flows subjected to adverse pressure gradient. The rich body of empirical information that the model contains gives it advantages over other models when applied to ‘complex’ boundary layers approaching separation, and this has made the model popular in aeronautical practice. Another interesting model is that of Menter (1997), the corner stone of which is also a transport equation for the turbulent viscosity. This arises from combination of the k- and ε-equations of a two-equation model with the constraint $-\overline{uv} = ak$, where

$a = (c_\mu^{1/2}) = 0.3$, which reflects experimental observations by Bradshaw et al. (1967). This constraint is extremely influential at high rates of strain. This can be recognised upon a consideration of the production rate in shear flow, into which the linear stress–strain relation is inserted, with the eddy-viscosity expressed in terms of k and ε:

$$P_k = -\overline{uv}\,\frac{\partial U}{\partial y};\ -\overline{uv} = c_\mu \frac{k^2}{\varepsilon}\left(\frac{\partial U}{\partial y}\right) \Rightarrow -\overline{uv} = c_\mu^{1/2}\sqrt{\frac{P_k}{\varepsilon}}\,k. \tag{3}$$

Thus, the constraint *limits* the shear stress to its equilibrium relationship to k.

In complex strain, away from the immediate vicinity of a wall, the turbulent length scale does not, nor is expected to scale with the wall distance. Neither is there, in general, any other global flow quantity (e.g. shear-layer thickness) which offers itself for scaling. Rather, the length scale must be expected to be governed by local turbulence mechanisms which evolve in space and time. This implies the need to determine the length scale from its own transport equation. This is, as it turns out, no mean task—one that is generally regarded as a major, if not the principal, obstacle to improving the predictive realism of turbulence models, not only within the eddy-viscosity framework, but also in the context of more elaborate closure approaches.

There are numerous proposals in the literature for two-equation models, many being variations of a few baseline models. One important issue is the quantity chosen to represent the length scale. Without exceptions, surrogate variables of the form $\zeta = k^n \varepsilon^m$ are used. While $\zeta = \varepsilon$ is the most obvious and popular option, it is one that causes significant problems in practice, especially in near-wall flows approaching separation. In computational aerodynamics, the most popular alternative to ε itself is the turbulent vorticity $\omega \equiv \varepsilon/k$ (Wilcox, 1988b, 1994) and, to a lesser extent, its inverse, the turbulent time scale τ (Speziale et al., 1992) and its root (Kalitzin et al., 1996). Models based on other length-scale equations include the $k^{1/2}$–$\xi(\xi = \varepsilon/k^{1/2})$ model of Gibson and Dafa'Alla (1995), k–R_t model of Goldberg (1994) and the k–L (or k–σ) model of Benay and Servel (2001).

A generic form of the dissipation-rate equation (Jones and Launder, 1972), used in conjunction with the k-transport equation and expression (1), is

$$\frac{\partial \varepsilon}{\partial t} + \frac{\partial U_j \varepsilon}{\partial x_j} = C_{\varepsilon 1}\frac{\varepsilon}{k}P_k + \frac{\partial}{\partial x_j}\left(\left(\frac{v_t}{\sigma_\varepsilon} + v\right)\frac{\partial \varepsilon}{\partial x_j}\right) - C_{\varepsilon 2}\frac{\varepsilon^2}{k}. \tag{4}$$

Its applicability to low-Reynolds-number near-wall flows necessitates the introduction of viscosity-related damping functions pre-multiplying c_μ and $C_{\varepsilon 1}$ or, more frequently, $C_{\varepsilon 2}$ and almost always of the form $(1 - \alpha \exp(-\beta Arg_\mu))$, where

$$Arg_\mu = \left\{ y^+ \equiv \frac{yu_\tau}{v},\ \ y^* \equiv \frac{yk^{1/2}}{v},\ \ R_t \equiv \frac{k^2}{v\varepsilon} \right\}.$$

It is the need for this (non-trivial) extensions and the introduction of additional terms, securing the correct wall-asymptotic behaviour, that has spawned numerous (about 20) model variations (Jones and Launder, 1972; Launder and Sharma, 1974; Hoffman, 1975; Lam and Bremhorst, 1981; Chien, 1982; Nagano and Hishida, 1987; Myong and Kasagi, 1990; So et al., 1991b; Coakley and Huang, 1992; Orszag et al., 1993; Kawamura and Kawashima, 1994; Lien and Leschziner, 1994).

In terms of predictive quality, there are rarely dramatic differences among aerodynamic quantities (except skin friction) returned by different variants of the k–ε model, unless particular ad hoc 'fixes' are introduced. The precise numerical values of the coefficients, especially $C_{\varepsilon 1}$ and $C_{\varepsilon 2}$, are of major importance to the predictive performance of two-equation models, and this has been the source of much uncertainty when trying to assess the inherent qualities of some model variations relative to others. Indeed, slight variations in the value of the coefficients are observed to be more influential than some major variations in the model formulation. Also of substantial influence are additive corrections, the best known being the so-called "Yap correction" and variations thereof (Yap, 1987; Jakirlić and Hanjalić, 1995), and curvature corrections, which sensitize at least one coefficient in the ε-equation to the "gradient" or "flux" Richardson number (Launder et al., 1977; Rodi, 1979; Rodi and Scheuerer, 1983), representing the intensity of curvature and its orientation relative to the strain.

Two-equation k–ε models are appropriate, in principle, for complex flows, do not involve fundamental restrictions in respect of flow features, including separation, and have been used extensively in aerodynamic computations. However, the overall conclusion emerging from extensive application experience is that they do not return high-quality results for conditions that are considerably more challenging than those in thin-shear-layer flows. In particular, the models have been observed to be too diffusive in stagnating flow, in boundary layers subjected to adverse pressure gradient and in the presence of stabilizing curvature—defects that result from a combination of the limitations of the eddy-viscosity concept and the tendency of the ε-equation to seriously overestimate the turbulent length scale and hence viscosity in decelerating near-wall flows. In consequence, separation from continuous surfaces tends to be seriously inhibited or delayed, recirculation regions are too short, skin friction is excessive and the wall-pressure variation is misrepresented. The many corrections and fixes proposed, none of which is general, bear witness to the inescapable conclusion that k–ε models constitute an insufficiently refined modelling framework for complex strain. On the other hand, for relatively simple thin shear flows, one- or even half-equation models can give as good, if not better, results that k–ε models at a considerably lower level of mathematical and numerical elaboration.

The difficulties experienced with k–ε models, in terms of predictive weaknesses and also numerical difficulties arising from the viscosity-affected near-wall properties of the ε-equation, have motivated efforts, especially in the 1990s, to formulate, test and improve models that use alternative length-scale variables, the most popular being the specific dissipation $\omega \equiv \varepsilon/k$ (Wilcox, 1988b, 1994). The choice of ω is initially curious, for its asymptotic variation is $\omega \rightarrow 2\nu/y^2|_{y\rightarrow 0} \rightarrow \infty$, a behaviour which requires the boundary condition to be specified at some finite distance from the wall. In contrast, its inverse has the natural and benign behaviour $\tau \rightarrow y^2/2\nu|_{y\rightarrow 0} \rightarrow 0$, and this has led Speziale et al. (1992) to recommend it over other length-scale variables.

The attraction of ω-based models is rooted in the observation that it gives a superior representation of the near-wall behaviour, especially in adverse pressure gradient. There are some fundamental arguments to support this. At the wall, the exact transport equation for ω can be shown to reduce to

$$\frac{2\nu}{k}\frac{\partial \omega}{\partial y}\frac{\partial k}{\partial y} + \nu\frac{\partial^2 \omega}{\partial y^2} + \omega^2 = 0, \tag{5}$$

which, in contrast to the ε-equation, does not contain higher-order turbulence correlations dependent on modelling assumptions. Substitution of the wall-asymptotic variation of ω, given above, and $(\partial k/\partial y) = (2k/y)$ into (5) shows wall-asymptotic consistency. Hence, ω also appears to be preferable to ε on that count. However, the practically influential issues lie elsewhere.

Thus, the modelled equation for ω, first proposed by Wilcox (1988b),

$$\frac{D\omega}{Dt} = C_{\omega 1}\frac{\omega}{k}P_k + \frac{\partial}{\partial x_j}\left(\left(v + \frac{v_t}{\sigma_\omega}\right)\frac{\partial \omega}{\partial x_j}\right) - C_{\omega 2}\omega^2, \tag{6}$$

with $C_{\omega 1} = 5/9$, $C_{\omega 2} = 5/6$, $\sigma_\omega = 2$, does not satisfy the wall-asymptotic behaviour and gives the wrong decay of k at the wall. This then led Wilcox (1994) to introduce damping functions pre-multiplying the eddy viscosity, the destruction term in the k-equation and $C_{\omega 1}$ in (6). However, the influence of these functions has been observed to extend, inapproriately, too far beyond the buffer layer, thus causing excessive damping and excessive sensitivity to adverse pressure gradient. Two other influential issues are, first, the role of the term $(\partial k/\partial x_j)(\partial \omega/\partial x_j)$, which distinguishes the ω-transformed ε-equation from the actual equation used, and second, the values of the coefficients. Starting from the k- and ε-equations, one can derive an equation for ω by inserting $\omega \equiv \varepsilon/k$ into the ε-equation, differentiating this and combining the result with the k-equation. Subject to the simplification $\sigma_k = \sigma_\varepsilon$, the outcome is

$$\frac{D\omega}{Dt} = (C_{\varepsilon 1} - 1)\frac{\omega}{k}P_k + \frac{\partial}{\partial x_j}\left(\frac{v_t}{\sigma}\right)\frac{\partial \omega}{\partial x_j} - (C_{\varepsilon 2} - 1)\omega^2 + \frac{2}{\omega\sigma}\frac{\partial k}{\partial x_j}\frac{\partial \omega}{\partial x_j}. \tag{7}$$

Comparison of (7) with (6) reveals the following differences:

- the ω-equation (6) lacks the mixed term in the transformed ε-equation (7);
- the coefficients of the production and destruction terms are 0.55 vs. 0.44 and 0.83 vs. 0.92, respectively;
- the Prandtl/Schmidt number in (7) is $\sigma \approx 1.3$, while $\sigma_\omega = 2$.

In addition, the Prandtl/Schmidt number in Wilcox's k-equation is 2, relative to 1 in the k–ε model. Hence, there are several potentially influential sources for the different performance of the k–ε and k–ω models. Although the coefficients of (6) satisfy equilibrium constraints implied by the log-law, the differences in the values can, on their own, be very influential. This is illustrated, for example, by Apsley and Leschziner (2000) for the case of a separated diffuser flow, in which the k–ω model was found to perform almost as poorly as the k–ε model.

One serious problem with the k–ω model is its extreme sensitivity to the value of ω at irrotational boundaries of shear flows (Menter, 1992a) and, by implication, also to the value in weak-shear regions within a complex shear flow. This, as well as other defects, have led Menter (1994) to formulate a hybrid model which blends the k–ω model near the wall with the k–ε in wall-remote regions. This is, currently, the most popular two-equation model in aeronautical CFD practice, especially in weakly separated flows. Computationally, the combination is effected via a weighted average formula operating on corresponding k–ε and k–ω model coefficients:

$$C_{\text{eff}} = FC_{k-\omega} + (1 - F)C_{k-\varepsilon}, \tag{8}$$

with F being a prescribed blending function, which ensures a dominance of the k–ω model in the region $y^+ < 70$ and the dominance of the k–ε beyond. An influential addition to the hybrid model is a correction which limits the shear stress in accordance with Bradshaw's relation $-\overline{uv} = ak$, the implication of which is expressed by Eq. (3). The limiter is introduced via

$$v_t = \frac{ak}{\max(\omega/a;\ \alpha\partial U/\partial y)}, \tag{9}$$

where $a = c_\mu^{1/2}$ and α is a function with extrema of 1 for boundary-layer flow and 0 for free shear flow. (Menter actually uses the vorticity Ω in place of the velocity gradient; these are identical in thin shear flow). The switch occurs at $c_\mu^{-1/2}\omega = \partial U/\partial y \rightarrow c_\mu^{-1/2} = (k/\varepsilon)(\partial U/\partial y) = -(\overline{uv}/k)$, which corresponds to the equilibrium condition $P_k/\varepsilon = 1$. Hence, in high strain, beyond the equilibrium state, (9) gives $v_t = \frac{c_\mu^{1/2}k}{\partial U/\partial y} \rightarrow -\overline{uv} = c_\mu^{1/2}k$.

This composite formulation—termed *shear–stress-transport* (SST) model—has enjoyed significant popularity in aerodynamic computations because of its favourable response to adverse pressure gradients. In a decelerating boundary layer, the limiter comes into action and reduces the shear–stress level relative to that of the non-limited k–ω model, and this is extremely effective in promoting separation, including shock-induced separation (Batten et al., 1999; Leschziner et al., 2001). In fact, it has been observed to be excessively effective in some separated flows, both subsonic (Apsley and Leschziner, 2000, 2001) and trans/supersonic flows (Liou et al., 2000) in which it gave too early separation and excessively long recirculation regions.

All models reviewed above use the turbulence energy k as the velocity scale in the eddy-viscosity relation. As turbulence is highly anisotropic, especially at a wall, k is not a particularly good representative of the velocity scale in the eddy-viscosity relation, if only because the shear stress in a shear layer is driven by the normal stress across that layer ($\overline{v^2}$ in a near-wall layer), as expressed by the exact production rate of the shear stress. This disparity is, in part, the reason for having to attach heavy damping to the eddy-viscosity, via the damping function f_μ, in two-equation models applicable down to the wall. As the wall is approached, anisotropy increases progressively, because the wall-normal intensity decays far more rapidly than the turbulence energy, with consequent rapid decline in shear–stress generation. This is a purely kinematic process, but one that cannot be captured properly via k, which decays far more slowly than $\overline{v^2}$. The damping function is introduced in compensation. However, its argument is the Reynolds number—that is, damping is assumed to be purely viscous, which is not consonant with reality. While viscous damping is effective, it is far weaker and occurs over a thinner region than is implied by the usual damping functions. These arguments form the basis for the "$V2$–f" model of Durbin (1995), which includes a transport equation for $\overline{v^2}$ instead of k and an additional wall-related "relaxation" equation, which 'relaxes' $\overline{v^2}$ towards k away from the wall. As the model leans heavily on closure ideas pertaining to Reynolds-stress-transport modelling, it will be reviewed later in the context of anisotropy-resolving models.

2.3. Anisotropy-resolving models

2.3.1. Second-moment closure

The natural modelling step beyond the eddy-viscosity framework, aiming especially at complex separated flows, is *second-moment closure*—that is, a model which consists of transport equations for all Reynolds stresses, without recourse to the artefact termed "eddy viscosity". A key advantage of second-moment closure is that the stress-generation terms do not require approximation, for they only involve products of stresses and strains. It is the stress-generation terms that are primarily responsible for the anisotropy and the selective response of turbulence to different strain types. Another advantage is that convective stress transport is represented exactly. Other processes require modelling, however, and this continues to be an active and challenging area of research.

The foundation of all RSMs is the exact set,

$$\underbrace{\frac{D\overline{u_i u_j}}{Dt}}_{C_{ij}} = -\underbrace{\left\{\overline{u_i u_k}\frac{\partial U_j}{\partial x_k} + \overline{u_j u_k}\frac{\partial U_i}{\partial x_k}\right\}}_{P_{ij}} + \underbrace{\left(\overline{f_i u_j} + \overline{f_j u_i}\right)}_{F_{ij}} - \underbrace{2\nu\overline{\frac{\partial u_i}{\partial x_k}\frac{\partial u_j}{\partial x_k}}}_{\varepsilon_{ij}}$$
$$+ \underbrace{\overline{\frac{p}{\rho}\left(\frac{\partial u_i}{\partial x_j} + \frac{\partial u_j}{\partial x_i}\right)}}_{\Phi_{ij}} - \underbrace{\frac{\partial}{\partial x_k}\left\{\overline{u_i u_j u_k} + \frac{\overline{p u_j}}{\rho}\delta_{ik} + \frac{\overline{p u_i}}{\rho}\delta_{jk} - \nu\frac{\partial \overline{u_i u_j}}{\partial x_k}\right\}}_{d_{ij}}, \tag{10}$$

in which C_{ij}, P_{ij}, F_{ij}, Φ_{ij}, ε_{ij} and d_{ij} represent, respectively, stress convection, production by strain, production by body forces (e.g. buoyancy $f_i = g_i \beta T'$), dissipation, pressure–strain redistribution and diffusion. The last three processes require modelling, and there is a large body of literature in this respect, of which only a small proportion is covered herein.

At high Reynolds numbers, away from the wall, dissipation is usually assumed to be isotropic, expressed by $\varepsilon_{ij} = \frac{2}{3}\varepsilon\delta_{ij}$. This approximation is inadequate close to the wall, where anisotropy in the small scales is substantial, and proposals have thus been made (e.g. in Gilbert and Kleiser, 1991; Launder and Tselepidakis, 1993; Hallbaeck et al., 1991; Hanjalić and Jakirlić, 1993) to sensitize ε_{ij}, in an algebraic fashion, to invariants of the stress anisotropy $A_2 = a_{ij}a_{ij}$; $A_3 = a_{ij}a_{jk}a_{ki}$; $A = 1 - \frac{9}{8}(A_2 - A_3)$, where $a_{ij} = (\overline{u_i u_j}/k - 2/3\delta_{ij})$ or the invariants $E_2 = e_{ij}e_{ij}$; $E_3 = e_{ij}e_{jk}e_{ki}$; $E = 1 - \frac{9}{8}(E_2 - E_3)$ of the dissipation anisotropy $e_{ij} = (\varepsilon_{ij}/\varepsilon - 2/3\delta_{ij})$. A model widely used to represents the anisotropic dissipation is

$$\varepsilon_{ij} = \frac{2}{3} f_\varepsilon \delta_{ij}\varepsilon + (1 - f_\varepsilon)\varepsilon^*_{ij}, \tag{11}$$

where ε^*_{ij} are the wall-limiting values of ε_{ij}, which can be readily obtained by applying Taylor-series expansions to the dissipation tensor in (11) (see Launder and Reynolds, 1983). The 'blending' function f_ε varies from model to model—there are at least 5 forms (see Hanjalić, 1994)—and its subjects are A and/or E and/or R_t. Apart from securing the correct wall-limiting behaviour of ε_{ij} and introducing shear–stress dissipation, proposal (11) also ensures that the dissipation of the wall-normal intensity is 'shut off' as turbulence approaches the two-component near-wall limit. This is an important element of any model designed to satisfy *realizability*, a property which includes the unconditional satisfaction of $\overline{u_\alpha^2} \geqslant 0$ (with α denoting the principal directions). More recent efforts (e.g. Oberlack, 1997) have focused on the derivation of transport equations for the dissipation components based on two-point correlation arguments, but such equations have not been used in aerodynamic practice.

The determination of the dissipation rate ε, required by (11), has already been the subject of discussion in relation to eddy-viscosity models. Much of what was said therein applies here too: the length-scale equation remains a major source of model weaknesses. With few exceptions, ε is determined from variants of the transport equation (4), with or without corrections (especially the "Yap correction" or variants thereof). The only major difference is the replacement,

$$\frac{\partial}{\partial x_j}\left(\frac{\nu_t}{\sigma_\varepsilon} + \nu\frac{\partial \varepsilon}{\partial x_j}\right) \leftarrow \frac{\partial}{\partial x_j}\left(c_\varepsilon \overline{u_j u_k}\frac{k}{\varepsilon}\frac{\partial \varepsilon}{\partial x_k}\right), \tag{12}$$

which implies that the diffusive flux of dissipation in any one direction is not simply associated with the gradient of the dissipation in that direction (a form of the Fourier–Fick law), but is a weighted sum of the gradients of the dissipation in all directions, each weighted by the appropriate Reynolds stress. This is referred to as the *Generalized Gradient Diffusion Hypothesis* (GGDH, Daly and Harlow, 1970), a concept also used to approximate stress diffusion:

$$d_{ij} = \frac{\partial}{\partial x_k}\left(c_s \overline{u_k u_l}\,\frac{k}{\varepsilon}\,\frac{\partial \overline{u_i u_j}}{\partial x_l}\right). \tag{13}$$

More complex forms than (13) exist, but are not demonstrably superior (see, for example, Demuren and Sarkar, 1993; Younis et al., 2000, for reviews) and have rarely been used. The rationale of the GGDH may be understood by reference to the exact transport equations for the triple correlations $\overline{u_i u_j u_k}$ (see Hanjalić and Launder, 1972). In the exact equations (10), the dominant fragment (at high Reynolds numbers) is $\partial(\overline{u_i u_j u_k})/\partial x_k$, with pressure diffusion being subordinate (estimated by Lumley (1978) at around 20%). It turns out that the triple-moment equations contain production terms that are formed as products of stresses and stress gradients. A simple algebraic model for the triple moments is one that is based on the assumption that these moments are proportional to their rate of generation multiplied by a turbulent time scale (k/ε). This notional relationship is reflected by (13).

Alongside dissipation, the redistribution or 'pressure–strain' term Φ_{ij} presents the modeller with the biggest challenge in the context of second-moment closure, and its importance is reflected by the large body of literature on the subject, which cannot be reviewed herein. This term vanishes upon the contraction $k = 0.5\overline{u_i u_j}\delta_{ij}$ (strictly, in incompressible flow only) and thus becomes irrelevant in closures based on the turbulence energy or a surrogate scalar. In second-moment closure, however, this term controls the redistribution of turbulence energy among the normal stresses—a process driving turbulence towards a state of isotropy—as well as the reduction in the shear stresses in harmony with the isotropisation process (recall Mohr's circle in solid mechanics). In simple shear flow, with flow direction x, the shear stress is driven by the y-directed normal stress $\overline{v^2}$, a (kinematic) stress that is not generated and is only finite because of the redistribution process effected by Φ_{22}. Moreover, Φ_{12} is the only term which balances the generation of shear stress and hence avoids that stress rising indefinitely.

Most models for the pressure–strain process rely on an analysis that shows, in principle, that the redistribution process consists of two major constituents, one involving an interaction between turbulent quantities only (Φ_{ij1} and referred to as the *slow* or the *Rotta* term) and the other involving an interaction between mean strain and turbulent fluctuations (Φ_{ij2} and termed *rapid*). This fact has led most modellers to make separate proposals for these two fragments, starting from the generic form,

$$\Phi_{ij} = \varepsilon A_{ij}(a_{ij}) + k M_{ijkl}(a_{ij})\frac{\partial U_k}{\partial x_l}, \tag{14}$$

in which the two terms represent, respectively, the *slow* and *rapid* processes. Simple forms are linear in the Reynolds stresses (Rotta, 1951; Hanjalić and Launder, 1972; Gibson and Launder, 1978; Fu et al., 1987b), but rely on a range of corrections to secure realizability and correct near-wall behaviour. In particular, the redistribution process needs to be sensitized to inhomogeneity, associated with large strain gradients, and to anisotropy invariants, especially in low-*Re* forms which allow the model to be used down to the wall (Launder and Shima, 1989; So et al., 1991a; Ince et al., 1994; Jakirlić and Hanjalić, 1995).

An alternative, proposed by Durbin (1993), introduces an *elliptic relaxation* equation of the form,

$$L^2\nabla^2 \frac{\Phi^c_{ij}}{k} - \frac{\Phi^c_{ij}}{k} = \frac{\Phi_{ij}}{k}, \tag{15}$$

where Φ^c_{ij} is the wall-corrected form of the standard (uncorrected) Φ_{ij}, L is the turbulence length scale and ∇^2 is the elliptic operator. Eq. (15) steers Φ_{ij} towards the correct wall values, prescribed as boundary conditions. Although this approach has been shown to perform well for several challenging flows (Durbin, 1993), it requires the solution of the 6 additional differential equations (15), which obviously adds to the resource requirements. A simplified variant of (15), intended for near-wall shear flows, is adopted as part of Durbin's (1995) so-called $V2$–f model and has already been mentioned at the end of Section 2.2 (f denotes the ratio Φ_{22}/k). The model involves a single Reynolds-stress equation for $\overline{v^2}$, essentially the stress normal to the wall or the streamlines. This stress is also the velocity scale used in the eddy-viscosity with which the mean flow is computed. The Reynolds-stress equation is solved in conjunction with the $i, j = 2, 2$ component of (15) and the k-equation.

From a fundamental point of view, as well as on practical grounds, the use of wall corrections is unsatisfactory, not only because of their non-general nature, but also because they rely heavily on the wall distance or wall-distance-related parameters. The latter is especially disadvantageous in complex geometries, where the influence of more than one wall needs to be taken into account, and when general non-orthogonal numerical grids are used. Hence, much of the recent fundamental research in the area of turbulence modelling has been concerned with the construction of *non-linear* pressure–strain models which satisfy the realizability constrains and do not require wall corrections. Non-linear models or variants have been proposed by Shih and Lumley (1985), Fu et al. (1987a), Speziale et al. (1991), Launder and Tselepidakis (1993), Craft et al. (1993), Craft (1998), Craft and Launder (1996), Pfunderer et al. (1997) and Batten et al. (1999), the last four being extensions of Fu et al.'s model and the very last being a compressibility-generalized variant suitable for shock-affected flows. The models differ in detail and in respect of the order of terms included, but all have arisen from the common approach of proposing non-linear expansions, in terms of components of the Reynolds-stress tensor $\overline{u_i u_j}$ (or rather the anisotropy tensor a_{ij}), to second- and fourth-rank tensors in Eq. (14). The coefficients of the various terms in the expansions for A_{ij} and M_{ijkl} are then determined by imposing necessary kinematic constraints (continuity, symmetry, etc.). Realizability is introduced into some model forms by sensitizing the pressure–strain model to invariants of the stress anisotropy. The most elaborate model is that of Craft and Launder (1996) and is quadratic in Φ_{ij1} and cubic in Φ_{ij2}, the latter containing six distinct groups of terms and associated coefficients. This model has recently been modified by Batten et al. (1999) to apply to shock-affected flows, in view of experience which had revealed that the parent form responds incorrectly to shocks. In common with linear models, the above cubic forms also rely on wall corrections (or *inhomogeneity* terms), albeit much weaker. Examples of parameters which express the wall influence without using the wall distance are: $f^w = (1/c_\mu^{-3/4}\kappa)(\partial l/\partial x_n)$ or $f^w = (1/c_\mu^{-3/4}\kappa)(\partial A^{1/2} l/\partial x_n)$, where $l = k^{3/2}/\varepsilon$ (Craft and Launder, 1996; Jakirlić, 1997).

The representation of low-Reynolds-number effects is yet another challenge, not dissimilar to that encountered in two-equation eddy-viscositry models. Most recent models, among them those of Shima (1988), Launder and Tselepidakis (1993), Launder and Shima (1989), So et al. (1991a), Jakirlić and Hanjalić (1995) and Craft and Launder (1996) are low-*Re* variants, allowing an integration through the viscous sublayer. This is an area in which much reliance is placed on recent DNS data for near-wall flows. In essence, different model elements, especially the dissipation equation (via $C_{\varepsilon 1}$, $C_{\varepsilon 2}$ and additive corrections to the equation), are sensitized to viscosity by way of damping functions with subjects being forms of the turbulent Reynolds number. As the near-wall structure is substantially affected by both inertial and viscous damping, the former provoking strong anisotropy via pressure reflections, low-*Re* extensions involve a functionalisation on anisotropy invariants as well as viscosity, each expressing a different physical process. In fact, the dissipation invariants can also be used, as has been done by Jakirlić and Hanjalić (1995). Because the functionalisation process is non-rigorous, essentially aiming to make the model return a phenomenological behaviour consistent with experimental or DNS data, there is a considerable amount of ambiguity in extending models to low-*Re* conditions, and thus each model features its own individual sets of functions derived along different routes. Such extensions are not, therefore, considered in detail here.

2.3.2. Non-linear eddy-viscosity and explicit algebraic Reynolds-stress models (NLEVM, EARSM)

A drawback of second-moment closure is its mathematical complexity and, arising from this, numerical difficulties and higher computational costs. In three-dimensional flow, the model consists of 6 highly coupled, non-linear partial differential equations, to which must be added at least one further equation for the rate of turbulence dissipation. If heat transfer or scalar transport is included, a consistent modelling framework entails the solution of (at least) 3 further equations for flux transport. In addition, the absence of the eddy-viscosity and of associated second-order gradient terms from both the mean-flow and Reynolds-stress equations tends to reduce the iterative robustness of most solution algorithms and adds to the computational costs. Finally, additional boundary conditions are required for the stresses (because they are transported). These are rarely available from experimental data and need to be inferred from other quantities. Yet, as will be demonstrated later, the above challenges can be and have been met for over a decade, and it is now possible to compute very complex 3D flows, both compressible and incompressible, with the most advanced forms of second-moment closure, incorporating non-linear models for the pressure–strain redistribution process and applicable down to the wall without Reynolds-number restrictions.

The complexities associated with second-moment closure have motivated efforts in recent years to construct simpler model forms which retain the principal advantages of the former over linear eddy-viscosity models. These have led to the formulation of a whole range of non-linear eddy-viscosity and explicit algebraic Reynolds-stress models, both consisting of sets of explicit algebraic relations for the stresses in terms of strains. These model are not as fundamentally firm as second-moment closure, but easier to implement and cheaper to apply.

NLEVMs are based on the general tensorial expansion,

$$a_{ij} = \sum_{\lambda} \alpha_\lambda T_{ij}^{\lambda}, \tag{16}$$

where T_{ij} is a function of the strain and vorticity tensors:

$$S_{ij} \equiv \frac{1}{2}\left(\frac{\partial U_i}{\partial x_j} + \frac{\partial U_j}{\partial x_i} - \frac{2}{3}\frac{\partial U_k}{\partial x_k}\right)$$

and

$$\Omega_{ij} \equiv \frac{1}{2}\left(\frac{\partial U_i}{\partial x_j} - \frac{\partial U_j}{\partial x_i} - 2\varepsilon_{ijk}\Omega_k\right),$$

in which Ω_k represents any system rotation, and the coefficients α_λ depend on the turbulent time scale (e.g. k/ε) and, in general, also on invariants of the strain and vorticity. Linear models follow, evidently, upon setting $\lambda = 1$, $T_{ij} = S_{ij}$, $\alpha_1 = -2\mu_t/k = -2c_\mu k/\varepsilon$. Following particular choices of (16), subject to tensorial constraints, the coefficients of the non-linear terms are determined by reference to experimental and DNS data for key baseline flows.

EARSMs turn out to have the same form as (16), but arise from an inversion of simplified forms of the Reynolds-stress-transport models discussed in the preceding section. The key simplification is Rodi's (1976) 'algebraic' approximation of the convective and diffusive stress transport,

$$\frac{D\overline{u_i u_j}}{Dt} - d_{ij} \approx \frac{\overline{u_i u_j}}{k}\left(\frac{Dk}{Dt} - d_k\right) = \frac{\overline{u_i u_j}}{k}\left(P_k - \varepsilon\right), \tag{17}$$

which leads to an implicit set of algebraic equations for the stresses, with the k- and ε-equations providing P_k and ε. The algebraic approximation for the convection in (17) is equivalent to $Da_{ij}/Dt = 0$, that is, the rate of change of the anisotropy vanishes, and the turbulence structure is thus assumed to be in equilibrium. Pope (1975) was the first to show that the algebraic set arising from the insertion of (17) into the model of Launder et al. (1975) could be arranged in the explicit form (16) (although P_k, which includes the stresses, was retained in its implicit form). The route by which EARSMs are derived will be indicated below. What should be clear already is the fact that both NLEVMs and EARSMs are inevitably less general and less fundamentally secure than full Reynolds-stress models. A particular problem arises from the fact that stress convection can be a substantial contributor to the stress balance in curved and swirling flows, and that, in such circumstances, turbulence-energy convection is not a good representation of the convection of stresses (see Fu et al., 1988). Generally, the adequacy of (17) is strongly dependent of the coordinate system adopted and the orientation of the flow relative to that coordinate system. Stress convection is only low in the streamwise direction, but the coordinates are very rarely well aligned with the flow in practically relevant flows. Some recent proposals designed to address this problem may be found in Girimaji (1997), Rumsey et al. (1999) and Wallin and Johansson (2001).

The derivation of expansions of the form (16) is constrained by the Cayley–Hamilton theorem, which dictates that there are at most 10 tensorially independent, symmetric, traceless, second-rank tensor products of S_{ij} and Ω_{ij} (Pope, 1975). No model contains all groups. Cubic models use the first 6 groups:

$$\begin{aligned}\mathbf{a} = \alpha\mathbf{s} &+ \beta_1(\mathbf{s}^2 - \tfrac{1}{3}\{\mathbf{s}^2\}\mathbf{I}) + \beta_2(\mathbf{ws} - \mathbf{sw}) + \beta_3(\mathbf{w}^2 - \tfrac{1}{3}\{\mathbf{w}^2\}\mathbf{I}) \\ &- \gamma_1\{\mathbf{s}^2\}\mathbf{s} - \gamma_2\{\mathbf{w}^2\}\mathbf{s} - \gamma_3(\mathbf{w}^2\mathbf{s} + \mathbf{sw}^2 - \{\mathbf{w}^2\}\mathbf{s} - \tfrac{2}{3}\{\mathbf{wsw}\}\mathbf{I}) - \gamma_4(\mathbf{ws}^2 - \mathbf{s}^2\mathbf{w}),\end{aligned} \tag{18}$$

where bold type is used for any 2nd-rank tensor, $\{\}$ indicates its trace, and $\mathbf{I} \equiv (\delta_{ij})$. Products are, for example, $\mathbf{ws} = \Omega_{ik}S_{kj}$ and $\mathbf{w}^2\mathbf{s} = \Omega_{ik}\Omega_{kl}S_{lj}$. The first term on the right-hand side corresponds to a linear eddy-viscosity model (stress $\propto$ strain). For simple shear, $\sigma = (k/\varepsilon)(\partial U/\partial y)$, (18) simplifies to:

$$a_{11} = \tfrac{1}{12}(\beta_1 + 6\beta_2 - \beta_3)\sigma^2, \quad a_{22} = \tfrac{1}{12}(\beta_1 - 6\beta_2 - \beta_3)\sigma^2, \quad a_{33} = -\tfrac{1}{6}(\beta_1 - \beta_3)\sigma^2, \tag{19}$$

and this shows that the quadratic terms allow normal-stress anisotropy to be captured. These terms make no contribution to the production of k in two-dimensional incompressible flow. The requirement that pure rotation should not generate anisotropy requires that β_3 is either identically zero or vanishes as $\mathbf{s} \to 0$. The terms with coefficients γ_1 and γ_2 are tensorially linear (proportional to $\mathbf{s}$) and are responsible for an important sensitivity to curvature, since in a curved shear layer,

$$\{\mathbf{s}^2\} + \{\mathbf{w}^2\} = -2\left(\frac{k}{\varepsilon}\right)^2 \frac{\partial U}{\partial R}\,\frac{U}{R}, \tag{20}$$

where R is the local radius of curvature. The γ_3-related term imparts a sensitivity to swirl. Both this and the γ_4-related term vanish in two-dimensional incompressible flow.

EARSMs are derived, in principle, by inserting (18) (or a variant thereof) into the implicit set of algebraic Reynolds-stress equations, which can be written in the form[1] : $\mathbf{a} = \mathrm{f}(\mathbf{a}, \mathbf{w}, \mathbf{s})$, where the right-hand side contains groups which are linear in $\mathbf{a}$, provided the pressure–strain process has been approximated by a linear model. This insertion then leads to a set of equations which can be solved for the set of coefficients in (18) (see, for example, Jongen and Gatski, 1998; Wallin and Johansson, 2000). Closure is then provided by equations for the turbulence scales, k and ε or ω. Apart from being constrained to linear pressure–strain models, EARSMs rely on the linearity of the dissipation to the stresses. This is irrelevant if the dissipation is assumed isotropic. However, more refined near-wall approximations, such as (11), with f_ε being a function of the stresses, present EARSMs with problems. These are addressed by Xu and Speziale (1996) and Johansson et al. (2000).

There are now about 15 NLEVMs and EARSMs. A first generation of quadratic models emerged through contributions by Saffman (1977), Wilcox and Rubesin (1980) and Speziale (1987). In Speziale's model, for example, the coefficients were simply taken to be powers of the time scale k/ε, so as to achieve dimensional consistency. Since then, a number of models of various complexity, derived along quite different routes, have emerged (Yoshizawa, 1987; Shih et al., 1993; Rubinstein and Barton, 1990; Gatski and Speziale, 1993; Craft et al., 1996; Lien and Durbin, 1996; Lien et al., 1996; Taulbee et al., 1993; Wallin and Johansson, 1997, 2000; Rung et al., 1999a; Apsley and Leschziner, 1998). Most NLEVMs are quadratic, while those of Craft et al., Lien et al., and Apsley and Leschziner are cubic. These differences in order are of considerable significance, especially in three-dimensional flows. In particular, the cubic fragments play an important role in capturing the strong effects of curvature on the Reynolds stresses.[2] The models by Shih et al., Lien et al., and Craft et al. are NLEVMs and start from the generic expansion (18), while those of Gatski and Speziale, Apsley and Leschziner, Taulbee et al., Wallin and Johansson and Rung et al. start from an algebraic Reynolds-stress model and are EARSMs. Other routes involve the *Direct Interaction* approximation adopted by Yoshizawa and the *Renormalisation Group* (RNG) approach taken by Rubinstein and Barton. Most models depend on two turbulence scales (usually k and ε) as well as strain and vorticity invariants. In contrast, one variant of Craft et al.'s cubic model makes use of a transport equation for the stress invariant $A_2 = a_{ij}a_{ij}$, while Lien and Durbin's quadratic model depends on the Reynolds stress normal to the streamlines, which is also obtained from a related transport equation.

[1] While implicit algebraic stress models can be and have been used directly, in which case they need to be inverted iteratively during the solution process, they tend to display numerical stiffness and have also been observed to generate more than one solution for one and the same flow, reflecting some ill-posedness.

[2] In 2D flow, the genuinely cubic fragments make no contribution. However, the quasi-cubic (strictly linear) terms in Eq. (18), associated with γ_1 and γ_2, are active. Indeed, these are responsible for imparting sensitivity to curvature, as reflected by Eq. (20).

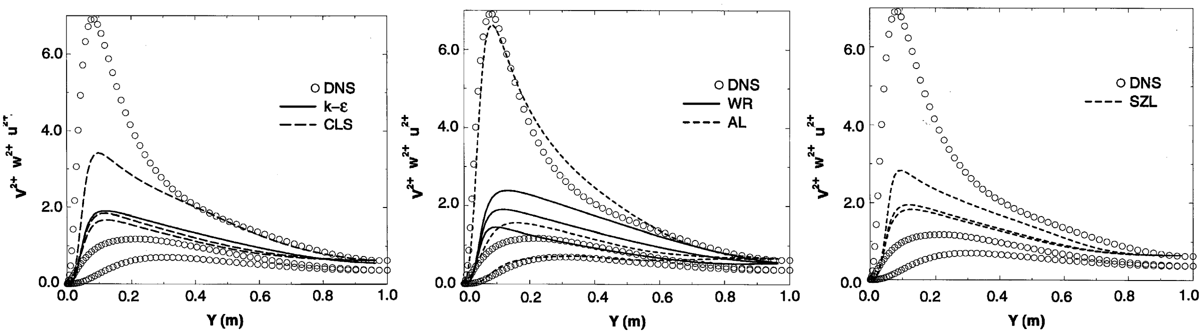

Fig. 1. Normal Reynolds stresses in fully-developed channel flow at $Re_\tau = 180$ predicted by four NLEVMs and the k–ε LEVM (taken from Loyau et al., 1998). Open circles denote DNS data, curves model predictions. The highest sets of circles and curves relate to u^{2+}, the middle sets to w^{2+} and the lowest sets to v^{2+}. The k–ε LEVM predicts isotropy; hence, only one curve relates to all three normal stresses.

As demonstrated through (19) and (20), NLEVMs are able to represent turbulence anisotropy and sensitivity to curvature. However, the realism with which they do so varies greatly. This is illustrated in Fig. 1, taken from Loyau et al. (1998) and comparing Reynolds-stress distributions returned by four non-linear models (AL=Apsley and Leschziner, CLS=Craft et al., WR=Wilcox and Rubesin, SZL=Shih et al.) for a fully-developed channel flow at $Re_\tau = 180$. The only one of the four that performs well is the AL model, and this reflects a careful near-wall calibration of the coefficients by reference to DNS data.

A recent model, formally designed to give the correct wall-asymptotic variations of the stress components, is that of Abe et al. (2003). This differs in two important respects from other models of the NLEVM type. First, it augments the basic quadratic constitutive stress–strain/vorticity equation by two additive fragments intended to account, respectively, for high normal straining and strong near-wall anisotropy. Second, it uses a form of the ω-equation that is much closer than Wilcox's form to the ε-equation. Specifically, it includes products of k and ω gradients and coefficients for the production and destruction terms that are directly equivalent to $C_{\varepsilon 1}$ and $C_{\varepsilon 2}$ normally used in the ε-equation. The modelling of near-wall anisotropy is based on the premise that this cannot be represented solely by the use of terms combining the strain and vorticity. The approach taken by Abe et al., thus to add a tensorially correct wall-related term to the constitutive stress–strain/vorticity relation is

$$a_{ij} \equiv \frac{\overline{u_i u_j}}{k} - \frac{2}{3}\delta_{ij} = f(S_{ij}, \Omega_{ij} \ldots),$$

which takes into account the wall orientation, represented by the wall-direction indicators $d_i = N_i/\sqrt{N_k N_k}$, where $N_i = \partial l_d/\partial x_i$ and $l_d = y_n$ (wall distance), which is then used in the additive wall-anisotropy correction of the form: ${}^w a_{ij} = -f_w \left(d_i d_j - \frac{\delta_{ij}}{3} d_k d_k\right) \times f(S_{ik}S_{kj}, S_{ik}\Omega_{kj}, S_{kj}\Omega_{ik}, S^2, \Omega^2 \ldots)$, where f_w is a viscosity-related damping function. In the above damping function, a composite time scale is used, which combines the macro-scale k/ε with the Kolmogorov scale $\sqrt{\nu/\varepsilon}$. The function then provides a smooth transition between the two scales across the near-wall layer. The performance of the model for the same flow as that in Fig. 1 is shown in Fig. 2 by reference to the mean velocity, Reynolds-stress components and dissipation rate. The turbulence-energy budget, not included here, is also very well predicted.

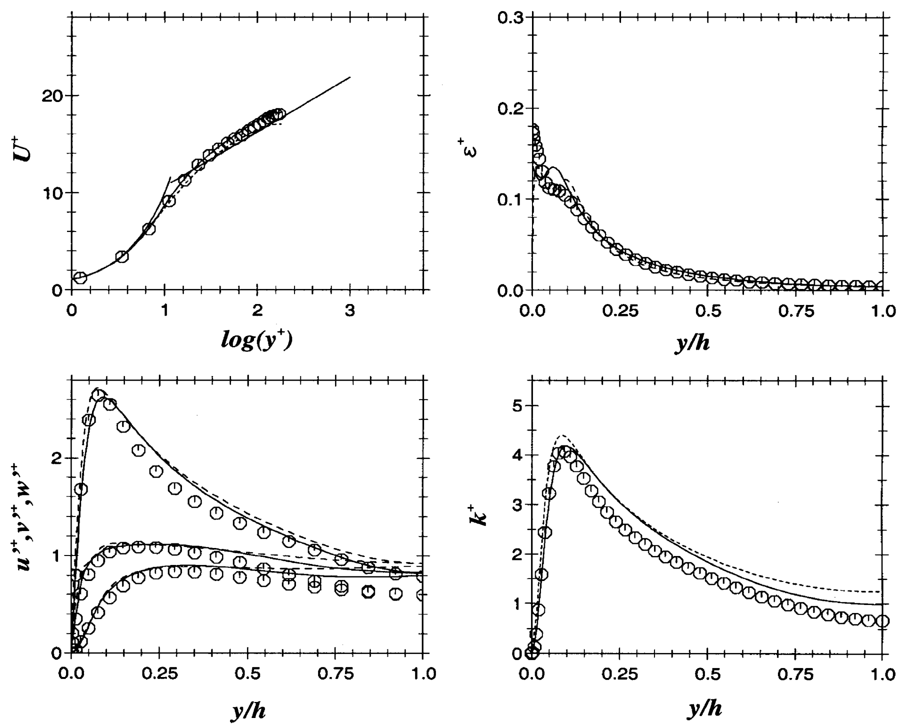

Fig. 2. Mean-velocity and turbulence-property profiles predicted by Abe et al. (2003) model for fully-developed channel flow at $Re_\tau = 180$. Two sets of curves are included, the solid lines relating to the model using the ε- and the dashed lines to the ω-equation. Symbols denote DNS data.

One problem which NLEVMs do not alleviate without intervention is the excessive generation of turbulence at high strain rates, which is one of the most serious defects of LEVM (unless containing realizability corrections). This problem is rooted in the form of the linear term in (18) if the coefficient α is taken to be $\alpha = -2c_\mu k/\varepsilon$, as would be consistent with the linear eddy-viscosity framework. This is not, of course, an issue relevant to EARSM, because they determine the coefficients from the Reynolds-stress model, which represents far better the sensitivity of the stresses and turbulence energy to the strain. A constant value of $c_\mu(=0.09)$ gives the wrong response to high strain rates (refer to the arguments accompanying Eq. (3)). The correct response implies the need for

$$c_\mu \propto \left(\frac{k}{\varepsilon}\frac{\partial U}{\partial y}\right)^{-1} \quad \text{or} \quad c_\mu \propto \left(\frac{k}{\varepsilon}S\right)^{-1}.$$

Substitution of the former into (3) shows $\overline{uv} \propto k$ (or $a_{12} = const.$), which is consistent with Bradshaw's expression $-\overline{uv} = ak$ and Menter's modelling proposal (9) for high strain rates. Loyau et al. (1998) show variations of c_μ with the non-dimensional strain in simple shear, $k/\varepsilon(\partial U/\partial y)$, built into several non-linear models, and illustrate a similar functional dependence, especially at strain rates exceeding the equilibrium value. In most model variants, c_μ is sensitized to both strain and vorticity invariants so as to also avoid the excessive generation of turbulence energy in stagnation flow. Such sensitization may, of course, also be applied to LEVMs, and this has indeed been done by Liou et al. (2000). Here again, EARSMs handle this type of sensitivity without special intervention.

2.4. Compressibility effects

Compressibility effects are, self-evidently, potentially important in aeronautical flow, many of which are at elevated Mach numbers. Compressibility manifests itself, first, through mean-density effects in all transport equations and, second, through turbulence correlations, associated with density fluctuations, which only arise in the presence of compressibility, and which require additional modelling assumptions. The approach taken has thus almost invariably been one of extending models, formulated and calibrated for incompressible flow, to compressible conditions.

Mean-density variations are accounted for explicitly, as a matter of course, in the computation of the convective as well as diffusive fluxes, the latter through dilatation terms in the constitutive stress–strain relation (1). Not normally accounted for, however, are implicit effects of density variations on the numerical values of the turbulence-model coefficients. Thus, Huang et al. (1994) show that satisfaction of the van Driest compressible log-law of the wall depends on the use of the ratio of local-to-wall densities in deriving the universal velocity. This has implications to the manner in which numerical constants in the turbulence-transport equations are derived by reference to experiments for incompressible flows. For example, the state of turbulence equilibrium, which is used to fix $C_{\varepsilon 1}$, depends, in compressible conditions, on the density gradients, and failure to account for this link leads to errors in the representation of the boundary-layer structure. One difficulty here is that every model variant, even within the same model category, exhibits a different level of sensitivity to the density gradient. Marvin and Huang (1996) show, for example, that the k–ω model is much less sensitive than the k–ε model to the density gradient, at least in terms of the log-law of the wall. Another problem is that the interaction of mean-density gradients with turbulence-model constants cannot really be divorced from other interactions associated with density fluctuations, for which explicit compressibility corrections are usually introduced. Hence, the effects of mean-density gradients need to be investigated with models which are complete, i.e. with all compressibility corrections included. Fortunately, implicit mean-density effects appear to be relatively unimportant when the Mach number is below 2–3.

Models for compressible flow are almost invariably expressed in terms of density-weighted (Favre) averaging. With this done, compressibility manifests itself explicitly by the appearance of dilatational pressure–strain and dilatational dissipation fragments in the Reynolds-stress equations, as well as source-like pressure-work terms which contain $\overline{u_k''}$, interpretable as a turbulent mass flux, with the double prime ($''$) denoting a density-weighted fluctuation. The three terms are written respectively, as:

$$\Phi_{ij}^{(d)} = \frac{2}{3}\overline{p\frac{\partial u_k}{\partial x_k}}\delta_{ij}, \quad \varepsilon_{ij}^{(d)} = \frac{8}{3}\overline{\nu s_{kk} s_{ij}}, \quad \bar{\rho}S_{ij}^{(P)} = -\bar{\rho}\overline{u_i''}\frac{\partial P}{\partial x_j} - \bar{\rho}\overline{u_j''}\frac{\partial P}{\partial x_i}. \tag{21}$$

There have been several proposals to approximate the dilatational terms, typically linking them quadratically to the turbulence Mach number (Zeman, 1990; Sarkar et al., 1991; Wilcox, 1993; Fauchet et al., 1997; Aupoix et al., 1986; Sarkar, 1992; Zeman, 1993; El-Baz and Launder, 1993). However, the analysis of DNS data by Huang et al. (1995) for supersonic boundary layers at $M = 1.5$ and 3 has demonstrated that the dilatational terms are not only insignificant in near-wall flows, in marked contrast to free flows, but that all major models for the dilatational terms grossly over-estimate their actual influence, and that the assumption of the dilatational dissipation being correlated with the turbulent Mach number is incorrect. Indeed, the effect of most compressibility corrections on turbulent boundary layers is in the wrong direction (Huang, 1990). It is not surprising, therefore, that the use of these models to predict compressible boundary layers gives disappointing results. Thus, the outcome of extensive validation studies in the 1990s at NASA for shock-affected boundary layers is encapsulated by the statement by Marvin and Huang (1996) that "indeed experience has shown that for the prediction of subsonic and supersonic flows, these two modifications degrade the results and are not recommended". The principal conclusion is, therefore, that there is no tenable argument for including any explicit compressibility models in computations of near-wall flows upto $M = O(5)$. What to do beyond this value is unclear at present. For free shear layers, current dilatation-related corrections are effective, but must be used with considerable caution in view of their probably serious fundamental flaws.

3. Model performance

It is not possible, within the constraints of this paper, to give a comprehensive review of application of turbulence models to aerodynamic flows, even for those featuring separation. There are numerous applications of one- and two-equation (and simpler) models to separated flows, despite all their frailties, but in many of these, the separated region is not large and often hugs the wall (i.e., is relatively long and thin). In such circumstances, the accuracy with which the details of the separated zone need to be resolved is not critical. Moreover, the flow in thin zones is tied to wall scales, as in a boundary layer, so that models designed for wall boundary layers can give a good representation, especially if the model has been carefully tuned to boundary layers in adverse pressure gradient approaching separation. This is the case, for example, with the SST model of Menter (1994) and the Spalart–Allmaras model (1992). Gerolymos and Vallet (1996) provide an overview table of over 30 computational studies of transonic flows with two-equation models (mostly k–ε), and comprehensive validation programmes are documented in Haase et al. (1993, 1996). A broad conclusion emerging from these is that models of this type, unless corrected, tuned to specific conditions or used with different constants relative to the base-line formation, generally return disappointing results in separation (although much better than algebraic models). This is especially so in separation from curved surfaces, in decelerating boundary layers, in curved shear layers and in shock/boundary-layer interaction. Better performance is returned when separation is provoked by sharp edges, such as in backward-facing steps.

There are a fair number of studies that report relatively modest performance differences between basic k–ε and k–ω formulations. A difficulty here is that any intrinsic differences between the ε- and ω-equations are clouded by the strong dependence of performance on the precise value of the numerical constants in the ω-equation, the nature of the viscosity-related damping functions and the inclusion or omission of the fragment of mixed k- and ω-derivatives (see Eq. (5)). For example, Jang et al.'s (2002) computations of the separated flow behind a streamwise periodic channel constriction show that the k–ω model yields significantly stronger sensitivity to adverse pressure gradient, hence giving a longer recirculation zone, but this appears to be linked, principally, to the viscosity-dependent damping functions.[3] There is ample evidence pointing to excessive near-wall turbulence is returned by both types of length-scale equation, thus hindering deceleration and separation, albeit to a different extent. Menter (1992b), Huang (1997)

[3] Substantial sensitivity has been observed to whether the 1988b or 1994 version of the ω-equation is used.

and Bardina et al. (1997) show this for Driver's (1991) incompressible separated boundary layer, the Bachalo–Johnson (1986) transonic-bump flow and the RAE 2822 aerofoil (Cook et al., 1979; Rung et al., 1999b) for Delery's separated bump flow, the RAE 2822 aerofoil and the ONERA M6 wing (Schmitt and Charpin, 1979); Apsley and Leschziner (2000) for the separated diffuser flow of Obi et al. (1993); Barakos and Drikakis (1998) for the Bachalo–Johnson transonic-bump flow; Barakos et al. (1999) for the subsonic flow around the Aerospatiale A aerofoil (Piccin and Cassoudesalle, 1987) and the transonic flow around the RAE 2822 aerofoil; Abid et al. (1995, 1996) for Coles and Wadcock's (1979) measurements of the flow around the NACA 4412 aerofoil, the RAE 2822 aerofoil and the axisymmetric bump flow. A similar message is conveyed in a compilation by Dolling (1998) of computational studies for compression ramps. Finally, Robinson and Hasan (1998) report a poor performance of the k–ω model for transonic flow over the RAE 2822 (Case 10) and NACA 0012 aerofoils and subsonic separation over the NACA 4412 aerofoil. These defects are partly rooted in fundamental weaknesses of the eddy-viscosity formulation and partly in the tendency of the length-scale equation to give excessive values for this scale. To this must be added the strong sensitivity of the k–ω model to the free-stream level of ω (Menter, 1992a; Bardina et al., 1997), which makes the model perform especially badly in free shear layers (Bardina et al., 1997). The use of the time scale τ as a surrogate length-scale equation in the models of Speziale et al. (1992) and Kalitzin et al. (1996) offers only marginal benefits, if judged on the basis of solutions for the separated flow over the Aerospatiale A high-lift aerofoil (Haase et al., 1996). In a study by Coakley and Huang (1992), 6 two-equation models have been applied to strong shock-wave/boundary-layer interaction on a cylinder-flare geometry and compression corners at Mach 2.84–9.22 (see also Dolling, 1998). While the models were found to give a wide range of performance in terms of separation and reattachment behaviour, the basic k–ω model was demonstrated to offer no intrinsic advantages over the k–ε framework. Similar conclusions are offered by Haidinger and Friedrich (1993, 1995), again for supersonic-ramp flows, although Coratekin et al. (1999) show that the inclusion of compressibility corrections to the k–ω model can substantially improve the model's predictive capabilities for ramp flows. The performance of various k–ε models for shock-induced separation in transonic bump, aerofoil and jet-afterbody flows is also deficient, as shown in Haase et al. (1993), Lien and Leschziner (1993), Zhou et al. (1995), Barakos and Drikakis (1998), Gerolymos and Vallet (1996) and Leschziner et al. (2001), among many others. All models again under-estimate the strength of interaction, failing to resolve separation and misplacing the shock. Broadly consistent conclusions also emerge from many studies of three-dimensional flows—for example in separated fuselage-like flows (Lien and Leschziner, 1997) and wing–body/junction flows, both subsonic (Apsley and Leschziner, 2001) and supersonic (Batten et al., 1999). Interestingly, the predictive defects in three-dimensional flows occasionally appear to be less serious than in two-dimensional ones, despite the added strain complexities involved (e.g. Robinson and Hassan's (1998) computations of shock/boundary-layer interaction over a cylinder/offset-flare juncture). This can be attributed, at least in some cases, to the larger contribution of convection to the balance of processes governing momentum transport, arising from a generally much larger flow curvature.

The addition of corrections to the basic two-equation-model form can have major consequences to the predicted behaviour. The "Yap" correction tends to slightly improve the prediction of k–ε models in adverse pressure gradients. The most influential correction is that of Menter (see Eq. (9)), which limits the shear stress by linking it to the turbulence energy, thus over-riding the eddy-viscosity relation. It will be recalled that Menter's model is a hybrid, combining the k–ε and k–ω models. This combination is not, in itself, a key feature. Of much greater importance is the shear–stress limiter, and several studies show the introduction of this limiter to result in a much improved behaviour in separated flows, including shock-induced separation in several transonic aerofoil and wing configurations (Huang, 1997; Marvin and Huang, 1996; Batten et al., 1999; Haase et al., 1996), jet-afterbody flows (Leschziner et al., 2001), incompressible aerofoil flows (e.g. Aerospatiale A and NLR 7301 two-element configuration, Haase et al., 1996) and dynamic stall in oscillating aerofoils (Srinivasan et al., 1993; Ekaterinaris and Menter, 1994). An excessive sensitivity of SST (*shear–stress-transport*)-model solutions to adverse pressure gradient for transonic-bump and supersonic compression-ramp flows is reported, however, by Liou et al. (2000). Flows in which the SST model does not work well include some complex three-dimensional configurations—for example, incompressible wing/body-junction flow (Apsley and Leschziner, 2001) and strong three-dimensional shock/boundary-layer interaction in a channel with a skewed bump (Leschziner et al., 2000b). In both cases, the SST model appears to return an insufficient level of stresses, resulting either in excessive separation or insufficient post-shock recovery, the latter leading to grossly excessive transverse motion in the recovery region.

Early applications of RSMs to aerospace-related problems were directed principally towards predicting shock/boundary-layer interaction, and were motivated by the poor performance returned by two-equation eddy-viscosity models. Studies by Vandromme and Ha Minh (1985), Benay et al. (1987), Leschziner et al. (1993), Lien and Leschziner (1993), Morrison et al. (1993), all concerned with shock-induced separation over nominally two-dimensional channel bumps and/or the RAE 2822 aerofoil, conveyed a broadly positive message on the predictive advantages gained from RSTMs relative to k–ε eddy-viscosity models. Thus, separation was found to be predicted at the correct position, the lambda-shock structure and the extent of the recirculation zone were better resolved, and the characteristic surface-pressure plateau associated with the separation zone was captured. It must be said that this outcome was no surprise to those familiar with the much more extensive earlier experience with RSTMs in predicting incompressible, mostly internal flows.

Over the past decade, there has been a steady, albeit slow, broadening in the range of conditions and problems computed with RSMs and, more recently, with non-linear eddy-viscosity models (NLEVMs). Some of the most complex flows investigated over the past three years with RSTM variants include shock/boundary-layer interaction in a Mach2 fin/body junction flow (Batten et al., 1999) and in a Mach1.8 jet injection into a Mach3 cross-flow (Chenault and Beran, 1998; Chenault et al., 1999), shock-induced separation in two- and three-dimensional jet-afterbody configurations (Leschziner et al., 2001) and over a swept bump in a channel (Gerolymos and Vallet, 1997), shock/boundary-layer interaction over a full body-wing-fin model of a generic fighter configuration (Leschziner et al., 2001) and dynamic-stall flows around aerofoils (Drikakis and Barakos, 2000). The additional challenge of predicting heat transfer with RSTMs, especially in hypersonic flow, has been addressed by Huang (1990) and Huang and Coakley (1993). Some recent applications of NLEVMs to aeronautical flows are those of Lien and Leschziner (1995, 1997), Loyau et al. (1998), Leschziner et al. (2000a,b), Hasan et al. (2001), Barakos and Drikakis (1998) and Apsley and Leschziner (2001). An overall conclusion arising from a variety of studies with NLEVMs and EARSMs, not only those pertinent to external aerodynamics, is that the performance of such models is considerably more variable than that of RSTMs. This is rooted, on the one hand, in major fundamental differences, in terms of derivation, between NLEVMs and EARSMs, and, on the other hand, in the high sensitivity of NLEVMs to the calibration process for the coefficients of the non-linear fragments in the stress–strain/vorticity relations. In addition, the performance of a NLEVM depends greatly on the order of terms included and the dependence of c_μ (or lack of it) on the strain and vorticity invariants, the latter being highly influential in relation to the response of the model to high strain rates. In fact, some studies suggest that the precise form of the dissipation-rate equation (especially the coefficients therein)

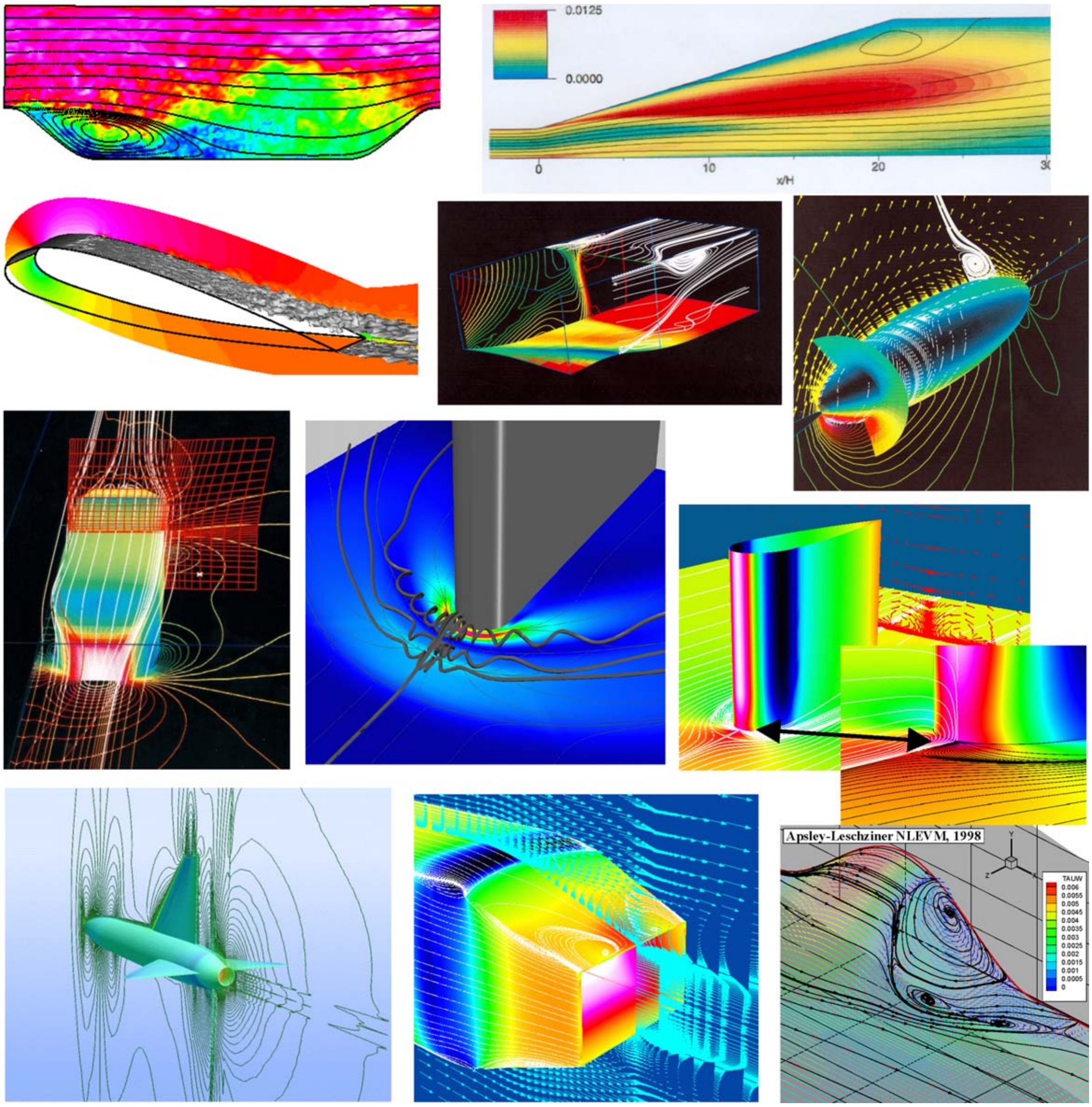

Fig. 3. Some separated flows investigated by the writer and his associates with anisotropy-resolving models.

and the form of c_μ carry more weight than the inclusion or exclusion of the higher-order terms that are responsible for the resolution of anisotropy and the sensitivity to curvature.

Fig. 3 provides a compilation of some of the separated flows that the writer and his collaborators have investigated over the past few years. A significant number are compressible, with separation being induced by strong shock waves. While these are obviously of substantial interest in the context of high-speed aerodynamics, they are, in fact, generally somewhat less challenging (unless confined) than low-speed flows, in which the separation occurs from curved surfaces and is thus more ill-defined, being induced by a much gentler adverse pressure gradient than that associated with a shock wave.

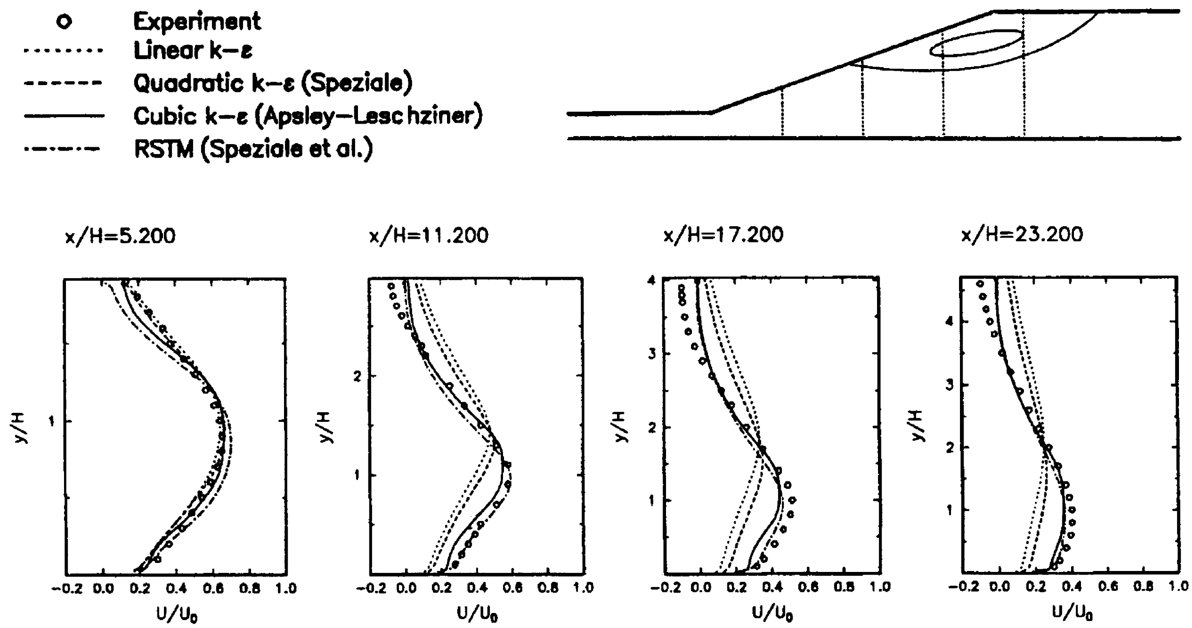

Fig. 4. Separated flow in an asymmetric diffuser; taken from Apsley and Leschziner (2000) (Measurements by Obi et al., 1993).

Computational results for three geometrically simple, but important and widely referred to test cases are given in Figs. 4–6. Although two of these are confined flows, both involve separation from continuous surfaces and are thus regarded as pertinent to the type of challenging conditions encountered in aerodynamic applications. In the asymmetric diffuser (Fig. 4) the challenge is to reproduce the strong asymmetry of the flow provoked by the deceleration and subsequent separation of the boundary layer along the inclined wall. This is seen to be predicted reasonably well by both the RSTM and cubic NLEVM used, in contrast to the linear k–ε EVM. The high-lift aerofoil shown in Fig. 5 has been the subject of extensive investigations, both with RANS models and LES (see Davidson et al., 2003, which documents the extensive Europe-wide collaborative study LESFOIL). This case has been found to defy LES, in so far as extremely costly calculations with many millions of nodes have failed to resolve the separation on the suction side. As seen from Fig. 5, anisotropy-resolving models do well, but the performance is observed to depend significantly on relatively small differences in the closure form, especially when NLEVMs are used.

Fig. 6 illustrates that the better fundamental footing of anisotropy-resolving closures and their tendency to predict a lower level of turbulence activity than (basic, i.e. ‘untuned’) LEVMs are not helpful in all circumstances, in so far as they do not always translate to better predictive performance. This applies, for example, to the first flow (top, l.h.s. plot) in Fig. 3: a periodic segment of a channel with constrictions that provoke massive separation. This is an exceptionally ‘rewarding’ test case, because the baseline data have been generated by highly resolved LES undertaken by Temmerman et al. (2003). It is also a highly taxing test case, because of the streamwise periodicity involved and the fact that a shift of δ in the position of the separation point translates to a change of about 7δ in the recirculation length—a ratio that emerges from both simulations and model solutions. This case has recently been examined by Jang et al. (2002)

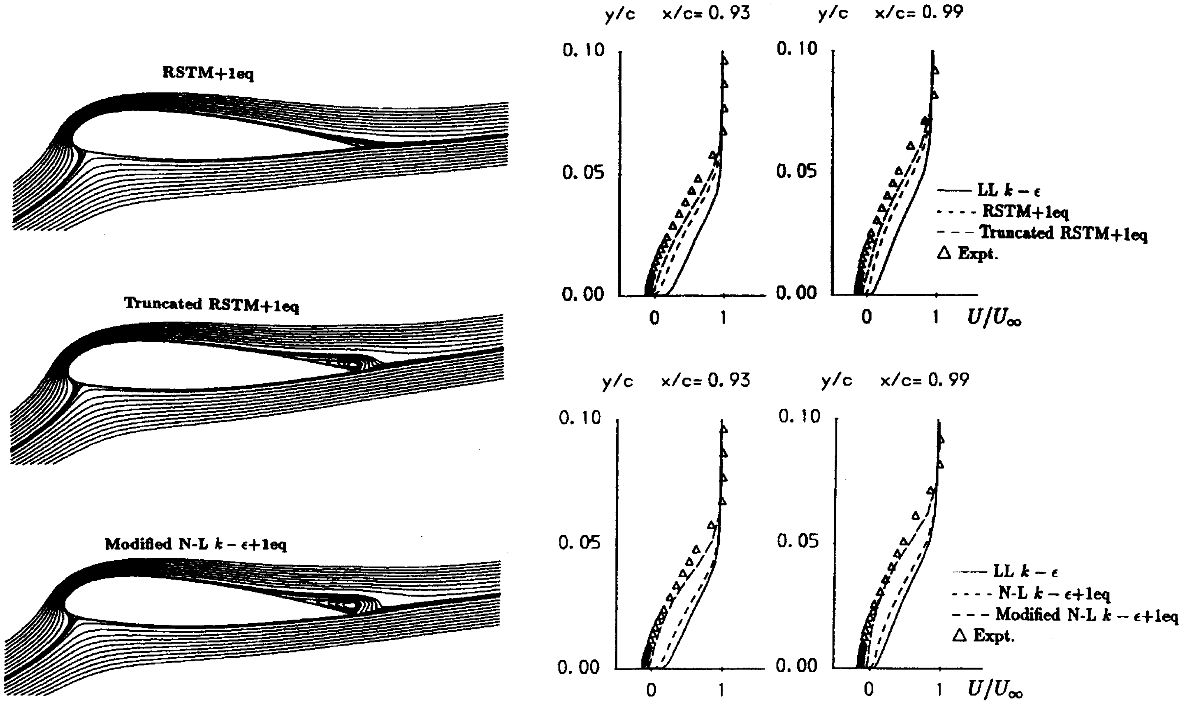

Fig. 5. Separated flow from a high-lift aerofoil; taken from Lien and Leschziner (1995) (Measurements by Piccin and Cassoudesalle, 1987).

using a wide range of NLEVMs, EARSMs and RSTMs. The flow has been computed both as a periodic configuration and as a sequence of 3 hill segments by Wang et al. (2004), with prescribed inlet conditions taken from the LES solution. The latter was done to examine the rate of approach of the flow to the periodic state. Fig. 6 gives an overall view of the flow (the upper l.h.s. plot is the LES result) as computed with several NLEVMs/EARSMs, but the study included a wide-ranging examination of turbulence properties, including the wall-asymptotic approach to the two-component state by reference to Lumley's "realizability map". As seen from Fig. 6, most NLEVMs give an excessively long recirculation zone, and even worse behaviour is observed with Menter's SST model (1994) and Spalart and Allmaras's one-equation model (1992), both highly tuned to separation and popular in aeronautical CFD. The conclusion emerging from this study is that all models display some important defects, with none giving a satisfactory description in all respects. However, of the models considered (among them second-moment forms not included herein), that by Abe et al. (2003) performed best (bottom r.h.s. plot in Fig. 6), especially in relation to the prediction of the anisotropy and of the wall-asymptotic approach of turbulence to the two-component state.

Model performance in 3D flows is illustrated by Figs. 7–12. The first application, now rather dated, is the flow around a prolate spheroid at 10° incidence (a 30° case has also been computed). Here, the main feature to capture is the vortical separation behind the body. Fig. 7 thus shows azimuthal-(or secondary) velocity profiles at the cross section 73% of the major axis behind the nose. This velocity is indicative of the intensity of the shed vortex. As seen, the RSTM predicts this velocity much better than the linear k–ε

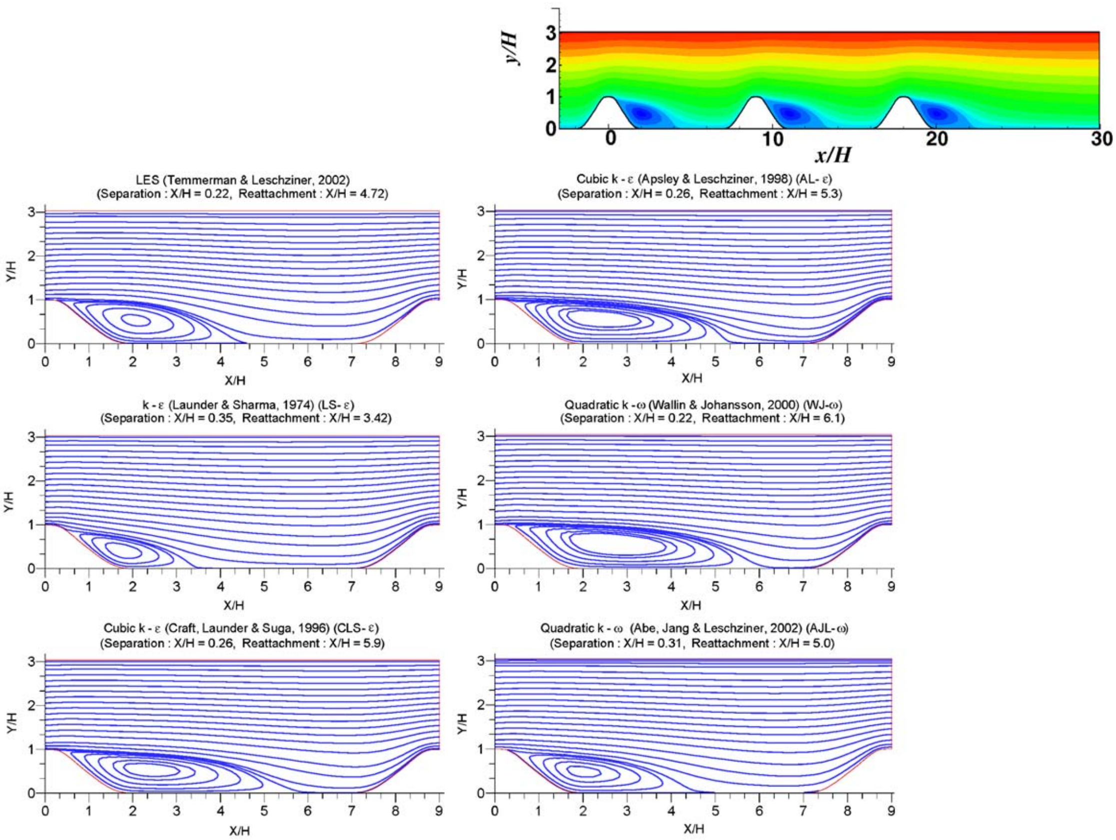

Fig. 6. Separated flow in a periodic duct segment with hill-shaped constrictions; streamwise contours; taken from Jang et al. (2002) and Wang et al. (2004).

EVM. At 30° incidence, natural transition plays an important role, and this makes the assessment rather more difficult. However, in that case too, indications are that the RSTM as well as the NLEVM perform better than the linear EVMs.

Figs. 8 and 9 show results for a flow around a wing–body junction. A vortex forms ahead of the wing nose (Fig. 9) and assumes a streamwise orientation as the flow progresses around the wing. This vortex forces lower-wall boundary layer upwards and free-stream fluid downwards towards the wall, mainly by convective transport. This process gives rise to the characteristic kidney-shaped contours of the streamwise velocity and turbulence quantities, seen in Figs. 8 and 9. The strength of the vortex is clearly decisive for the degree to which the contours are distorted, and both figures show that RSTMs and the NLEVM of Abe et al. represent the effects of the vortex well. In fact, this NLEVM has been found to perform substantially better than other NLEVMs examined (see Apsley and Leschziner, 2001, for results for two other NLEVMs), and this is due primarily to the ability of the model to resolve faithfully the separation process upstream of the wing nose.

Computational results for two compressible, shock-affected flows are given in Figs. 10 and 11. Both are highly pertinent to high-speed aerodynamics. In the first, the interaction with an external transonic flow

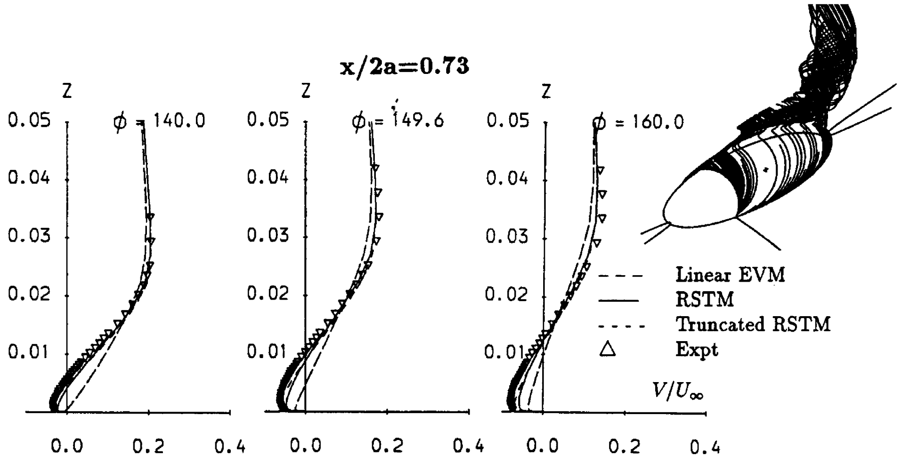

Fig. 7. Separated flow from a prolate spheroid at high incidence; profiles are for azimuthal velocities within the leeward vortex; taken from Lien and Leschziner (1997) (Experiments by Meier et al., 1984).

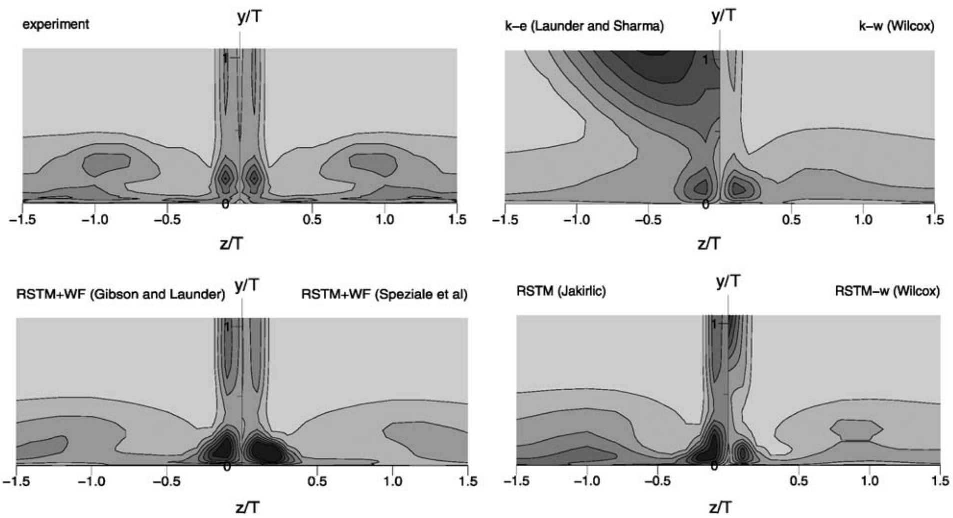

Fig. 8. Flow around a wing–body junction; contours of streamwise normal stress across a downstream plane computed with RSTMs; taken from Apsley and Leschziner (2001) (Experiments by Fleming et al., 1993).

(at free-stream Mach number 0.94) with an under-expanded jet causes a shock to form on the afterbody. This leads to separation, which is clearly visible on the outer nozzle wall in the inset in Fig. 10 (note the skin-friction lines on the upper wall). Solutions are included for two RSTMs (one, denoted by 'MCL', is the most advanced 'cubic' form in existence) and a cubic NLEVM. Both give a much better representation of the pressure field around the afterbody than the linear k–ε model. However, the SST model also provides a satisfactory solution, and this reflects the particular separation-related elements of the model referred to repeatedly in the discussion above.

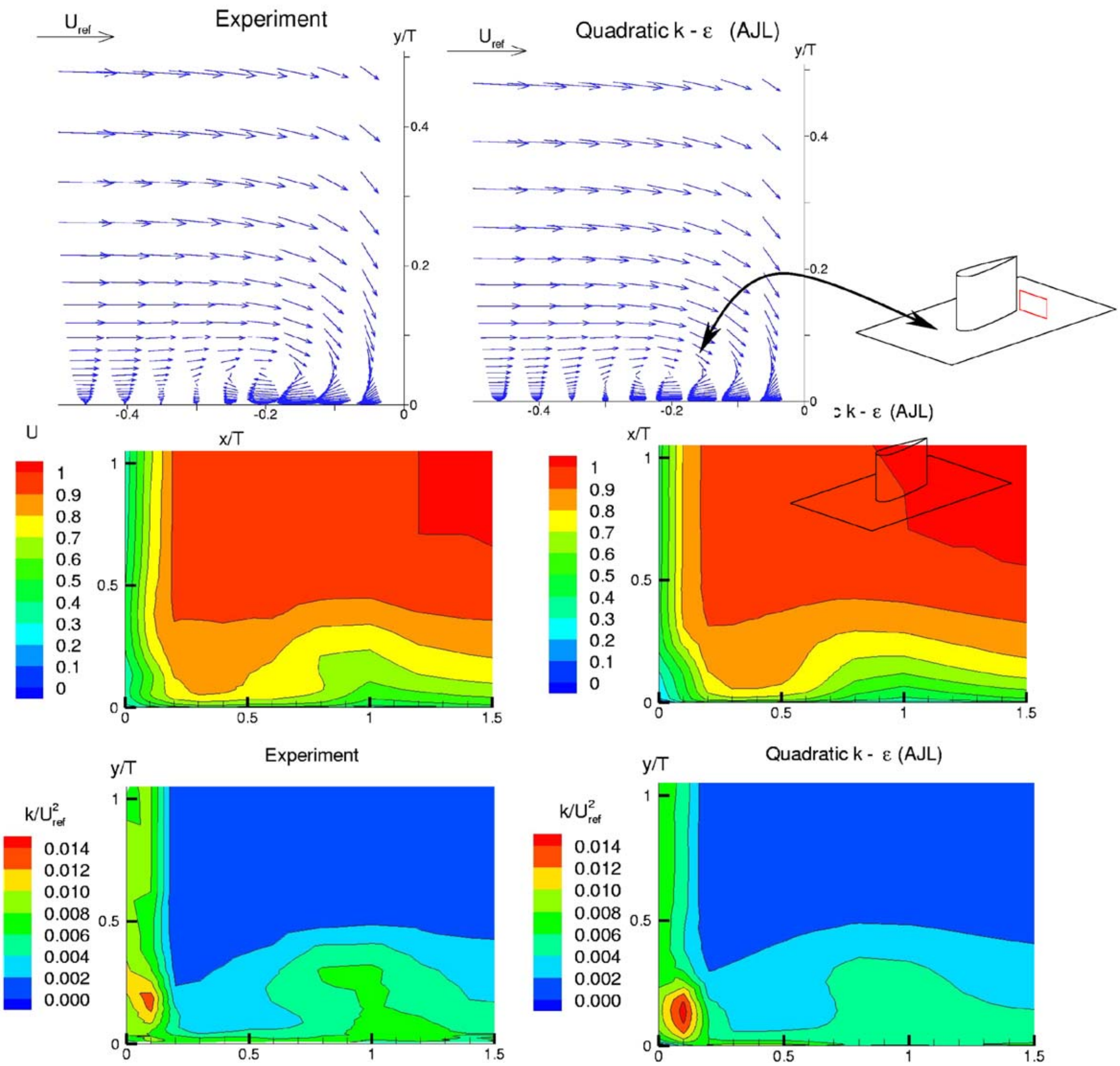

Fig. 9. Flow around a wing–body junction; velocity field ahead of wing nose and contours of streamwise velocity and turbulence energy across a downstream plane, computed with Abe et al.'s NLEVM; taken from Jang and Leschziner (unpublished data) (Experiments by Fleming et al., 1993).

The flow around the fin in Fig. 11 is especially complex. A strong bow shock causes a triple vortex to form, the two major components of which are seen in the upper r.h.s. plot which relates to the 'cubic' RSTM used. The lower plots in Fig. 11 provide comparisons between the experimental topology map and those produced by two RSTMs and the SST model. While the latter correctly returns the primary separation line, it does not resolve, in contrast to the RSTMs, the complex structure of the vortex. Again, the performance of the SST model reflects its tuning to separated flow, which in other cases gives rise to premature separation and delayed recovery.

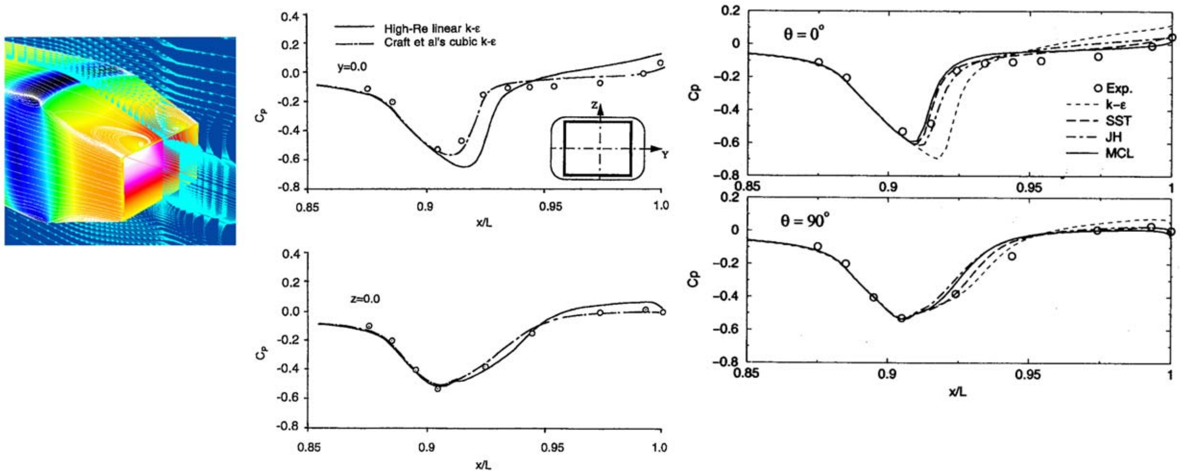

Fig. 10. Shock-induced separation on jet-afterbody computed with RSTM and NLEVM (taken from Leschziner et al., 2001; Hasan et al., 2001; Experiments by Putnam and Mercer, 1986).

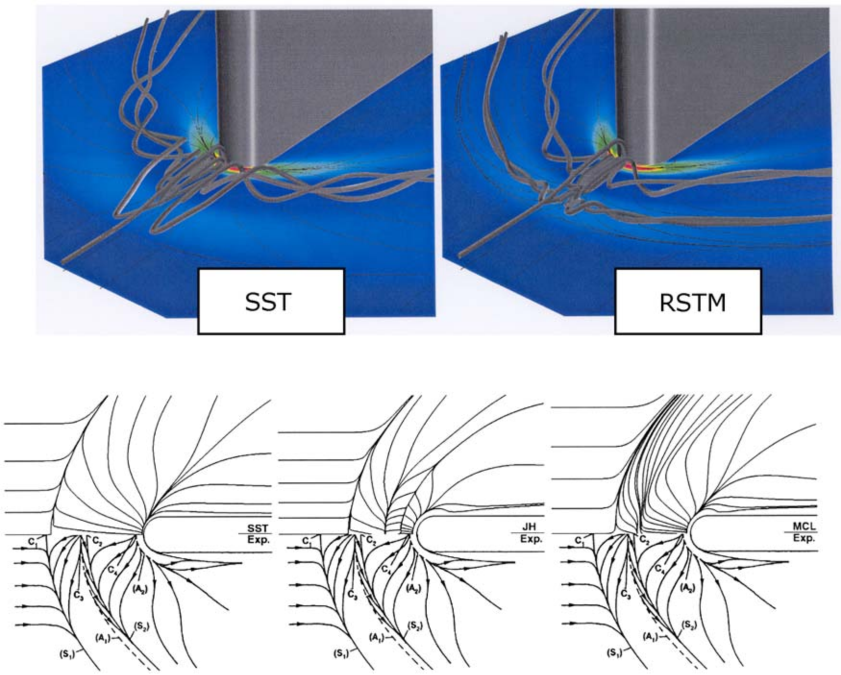

Fig. 11. Mach 2 flow around a fin-plate junction computed with RSTM and SST model (linear EVM) of Menter; upper figure vortex structure; lower figure lower-wall flow topology; taken from Batten et al. (1999) (Experiments by Barberis and Molton, 1995).

A final 3D validation example is shown in Fig. 12. This is a separated flow around a ducted 3D hill, with the boundary-layer thickness upstream of the hill being approximately 50% of the hill height. This is a difficult case for several reasons, not least because computational inlet conditions needed to be generated

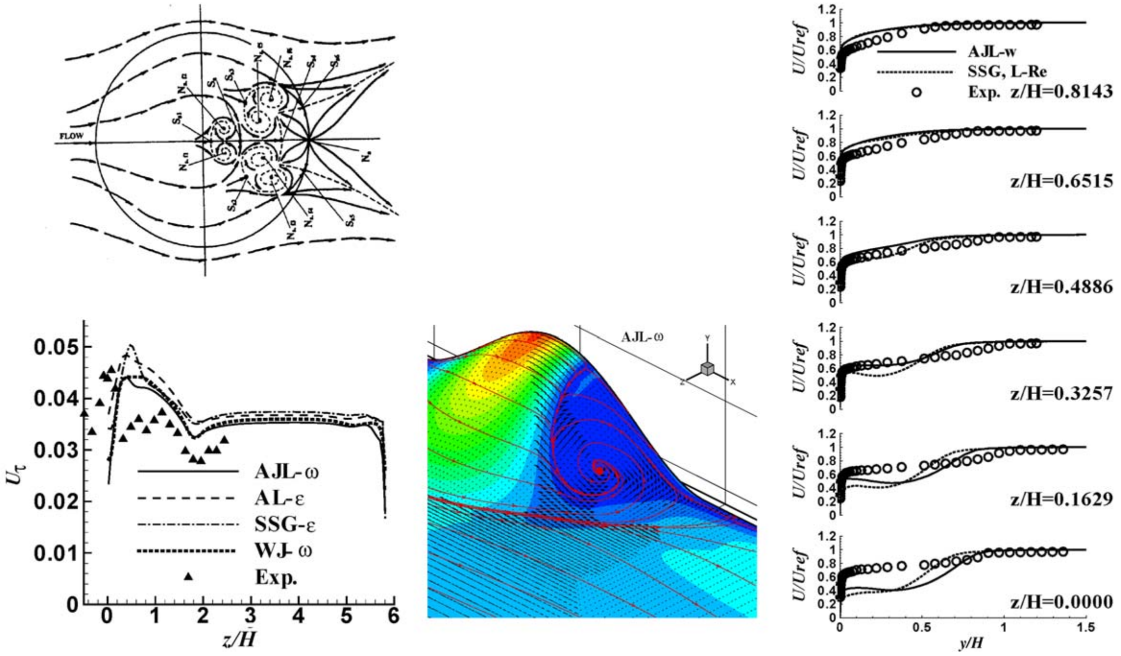

Fig. 12. Flow around a 3D hill; experimental vs. RSTM- and NLEVM-computed flow topology maps, friction velocity and streamwise velocity profiles at 3.7 hill heights downstream of hill crest; taken from Wang et al. (2004) (Experiments by Simpson et al., 2002).

precursor calculation for a duct without the hill. Also, the flow is characterised by severe skewing at the wall, followed by 'open' vortical separation. Fig. 12 shows results for four models, two being NLEVMs (AJL, AL), one EARSM (WJ) and the forth a RSTM (SSG). None is found to give a credible representation of the flow. The experimental topology map indicates the presence of three pairs of vortices on the leeward hill side, while all computations return a single pair. Although the experimentors have recently indicated that they believed their topology maps to be wrong and the actual structure to have a single pair, there clearly remain significant differences between LDA-measured and computed field variables. The results suggest above all that the real wake following separation fills and recovers at a much faster rate than predicted. LES computations recently performed for this geometry, but at a Reynolds number of only 10% of the experimental value (130,000), gave results which agreed well with corresponding RSTM solutions (Temmerman et al., 2004). Hence, the nature of the discrepancies observed in Fig. 12 remain unclear at the time of writing.

4. Concluding Remarks

The principal question which this article has addressed is whether current models are able to predict separation, especially from curved surfaces, with sufficient accuracy. The answer is a qualified *No*. There is ample evidence that eddy-viscosity models, unless modified in particular non-general ways, often perform poorly in flows featuring separation, strong shock/boundary-layer interaction and 3D vortical structures. More seriously, perhaps, the models do not display a consistent behaviour across a wide range of conditions. In relatively simple flows which develop slowly and in which a single shear stress (expressed in wall-oriented coordinates) is wholly dominant, eddy-viscosity models can be so constructed as to give the correct level of this stress and thus to yield adequate solutions. This applies to near-wall flows, thin wakes and even separated flows in which the separated region is long and thin and hugs the wall. Another type of flow in which eddy-viscosity models are adequate is one in which inviscid features (pressure gradient, advection) dictate the mean flow, so that the Reynolds stresses are largely immaterial, however wrong they may be. The fact that many flows are an amalgam of shear layers and regions in which turbulence is dynamically uninfluential explains, in part, the moderate level of success of eddy-viscosity models. Among two-equation eddy-viscosity models the SST form performs fairly well (at least in 2D flow), due to the limiter which prevents the shear stress from responding to the strain to the extent dictated by the stress–strain relationship. The length-scale equation is a key area of uncertainty, and its precise form greatly affects model performance. There is some evidence that models using the turbulent vorticity as a length-scale variable near the wall perform (marginally) better than models based on the dissipation-rate equation, although it must be stressed that performance depends greatly on the nature of viscosity-related damping functions and the numerical constants in the length-scale equation.

Much of the recent research in turbulence modelling has focused on the development of anisotropy-resolving models. Of these, Reynolds-stress-transport models are the most ‘complete’ and fundamentally secure forms, in the sense that they come closest to the exact representation within the constraints of closure at second-moment level. These models are complex and pose particular numerical challenges, but are now used to compute flows around practical configurations. The weak elements of such models are the length-scale equation and the (influential) pressure–strain model. While Reynolds-stress models often give better predictions than eddy-viscosity models in many complex ‘laboratory’ flows, they cannot be said to guarantee better solutions in practice. Current forms are therefore unlikely to be adopted in general industrial methods, except for analysing a narrow range of complex flow problems in a pre-design environment. Non-linear eddy-viscosity models are, at best, approximations of Reynolds-stress transport models—these forms being referred to as Explicit Algebraic Reynolds-stress Models (EARSMs). Hence, clearly, their performance cannot be superior to that of their parents. In particular, EARSMs ignore stress transport and are based on relatively simple (linear) closure forms for the dissipation rate and pressure–strain process. They are, however, numerically simpler and more economical than stress-transport closure and are therefore gaining in popularity. The performance of NLEVMs greatly depends on their derivation and calibration, and this explains their variable performance. Again, the length-scale equation plays a crucial role, but predictive differences are also due to substantial differences in the ability of the models to correctly return the anisotropy, especially at wall, and the response to different types of strain.

Is Large Eddy Simulation a panacea, to replace RANS? The answer is an emphatic *No*. LES undoubtedly offers clear predictive advantages in bluff-body aerodynamics in which large-scale unsteadiness is a key feature. It performs well when separation is provoked at sharp edges and when the principal features of interest are associated with shear layers remote from walls and are not affected by viscous wall processes. LES is much more problematic in near-wall flows, especially when wall curvature induces separation. LES continues to be very costly, typically two orders of magnitude higher than RANS, places considerably more stringent constraints than RANS on numerical accuracy and grid quality, and requires the spectral content of boundary conditions to be specified. While LES will increasingly be used in practical applications, it is unlikely to replace RANS, especially for near-wall flows. The Detached Eddy Simulation (DES) method of Spalart et al. (1997), or a related strategy, may be a possible route to economically tenable simulations for complex configurations, but there are several important fundamental and practical questions that need to be addressed and resolved in relation to the coupling of near-wall RANS models to the outer LES region, on which DES is based.

References

Abe, K., Jang, Y.-J., Leschziner, M.A., 2003. An investigation of wall-anisotropy expressions and length-scale equations for non-linear eddy-viscosity models. Int. J. Heat Fluid Flow 24, 181–198.

Abid, R., Rumsey, C., Gatski, T.B., 1995. Prediction of non-equilibrium turbulent flows with explicit algebraic stress models. AIAA J. 33, 2026–2031.

Abid, R., Morrison, J.H., Gatski, T.B., Speziale, C.G., 1996. Prediction of aerodynamic flows with a new explicit algebraic stress model. AIAA J. 34, 2632–2635.

Apsley, D.D., Leschziner, M.A., 1998. A new low-Reynolds-number nonlinear two-equation turbulence model for complex flows. Int. J. Heat Fluid Flow 19, 209–222.

Apsley, D.D., Leschziner, M.A., 2000. Advanced turbulence modelling of separated flow in a diffuser. Flow, Turbulence Combustion 63, 81–112.

Apsley, D.D., Leschziner, M.A., 2001. Investigation of advanced turbulence models for the flow in a generic wing–body junction. Flow, Turbulence Combustion 67, 25–55.

Aupoix, B., Blaisdell, G.A., Reynolds, W.C., Zeman, O., 1986. Modelling the turbulent kinetic energy equation for compressible homogeneous turbulence. AIAA J. 24, 437–443.

Bachalo, W.D., Johnson, D.A., 1986. Transonic turbulent boundary layer separation generated on an axisymmetric flow model. AIAA J. 24, 437–443.

Barakos, G., Drikakis, D., 1998. Assessment of various low-Re turbulence models in shock boundary layer interaction. Comput. Methods Appl. Mech. Eng. 160, 155–174.

Barakos, G., Drikakis, D., Lefebre, W., 1999. Improvement to numerical predictions of aerodynamic flows using experimental data assimilation. J. Aircr. 36 (3), 611–614.

Barberis, D., Molton, P., 1995. Shock wave-turbulent boundary layer interaction in a three-dimensional flow. AIAA Paper 95-0227.

Bardina, J.E., Huang, P.G., Coakley, T.J., 1997. Turbulence modelling validation. AIAA Paper 97-2121.

Batten, P., Craft, T.J., Leschziner, M.A., Loyau, H., 1999. Reynolds-stress-transport modelling for compressible aerodynamic flows. AIAA J. 37, 785–796.

Benay, R., Servel, P., 2001. Two-equation k–σ turbulence model: application to supersonic base flow. AIAA J. 39, 407–416.

Benay, R., Coet, M.C., Delery, J., 1987. A study of turbulence modelling in transonic shock-wave/boundary-layer interactions. In: Proceedings of the 6th Symposium on Turbulent Shear Flows.Toulouse, pp. 8.2.1–8.2.6.

Bradshaw, P., Ferris, D.H., Atwell, N.P., 1967. Calculation of boundary layer development using the turbulent energy equation. J. Fluid Mech. 23, 31–64.

Cambon, C., Scott, J.F., 1999. Linear and nonlinear models of anisotropic turbulence. Ann. Rev. Fluid Mech. 31, 1–53.

Chenault, C.F., Beran, P.S., 1998. K-e and Reynolds stress turbulence model comparisons for two-dimensional injection flows. AIAA J. 36, 1401–1412.

Chenault, C.F., Beran, P.S., Bowersox, R.D.W., 1999. Numerical investigation of supersonic injection using a Reynolds-stress turbulence model. AIAA J. 37, 1257–1269.

Chien, K.Y., 1982. Predictions of channel and boundary-layer flows with a low-Reynolds-number turbulence model. AIAA J. 20 (1), 33–38.

Coakley, T.J., Huang, P.G., 1992. Turbulence modelling for high speed flows. AIAA Paper 92-0436.

Coles, D., Wadcock, A.J., 1979. Flying hot-wire study of flow past a NACA 4412 airfoil at maximum lift. AIAA J. 17, 321–328.

Cook, P.H., McDonald, M.A., Firmin, M.C.P., 1979. Aerofoil 2822—Pressure distributions, boundary layer and wake measurements. AGARD AR-138.

Coratekin, T., Schubert, A., Ballmann, J., 1999. Assessment of eddy-viscosity models in 2D and 3D shock/boundary-layer interactions. In: Rodi, W., Laurence, D. (Eds.), Engineering Turbulence Modelling and Experiments, vol. 4. Elsevier, Amsterdam, pp. 649–658.

Craft, T.J., 1998. Developments in a low-Reynolds-number second-moment closure and its application to separating and reattaching flows. Int. J. Heat Fluid Flow 19, 541–548.

Craft, T.J., Launder, B.E., 1996. A Reynolds stress closure designed for complex geometries. Int. J. Heat Fluid Flow 17, 245.

Craft, T.J., Graham, L.J.W., Launder, B.E., 1993. Impinging jet studies for turbulence model assessment—II. An examination of the performance of four turbulence models. Int. J. Heat Mass Transfer 36, 2685.

Craft, T.J., Launder, B.E., Suga, K., 1996. Development and application of a cubic eddy-viscosity model of turbulence. Int. J. Num. Methods Fluids 17, 108–115.

Daly, B.J., Harlow, F.H., 1970. Transport equations in turbulence. Phys. Fluids 13, 2634–2649.

Davidson, L., Cokljat, D., Froelich, J., Leschziner, M.A., Mellen, C., Rodi, W. (Eds.), 2003. LESFOIL: Large Eddy Simulation of Flow a High-Lift Airfoil, Notes on Numerical Fluid Mechanics and Multidisciplinary Design, vol. 83, Springer, Berlin.

Demuren, A.O., Sarkar, S., 1993. Perspective: systematic study of Reynolds-stress closure models in the computation of plane channel flows. ASME J. Fluids Eng. 115, 5–12.

Dolling, D.S., 1998. High-speed turbulent separated flows: consistency of mathematical models and flow physics. AIAA J. 36, 725–732.

Drikakis, D., Barakos, G., 2000. Numerical developments in unsteady aerodynamic flows, CD-Rom Proceedings of the ECCOMAS Conference, Forum: CFD in Aeronautics, Industrial Technology Session, EU, Barcelona.

Driver, D.M., 1991. Reynolds shear stress measurements in a separated boundary layer. AIAA Paper 91-1787.

Durbin, P.A., 1993. A Reynolds stress model for near-wall turbulence. J. Fluid Mech. 249, 465.

Durbin, P., 1995. Separated flow computations with the k–ε–v^2 model. AIAA J. 33, 659–664.

Ekaterinaris, J.A., Menter, F.R., 1994. Computation of oscillating airfoil flows with one- and two-equation turbulence models. AIAA J. 32, 2359–2365.

El Baz, A.M., Launder, B.E., 1993. Second-moment modelling of compressible mixing layers. Engineering Turbulence Modelling and Experiments, vol. 3, Elsevier, Amsterdam, pp. 63–70.

Fauchet, G., Sho, L., Wunenberger, R., Bertoglio, J.P., 1997. An improved two-point closure for weakly compressible turbulence and comparison with large-eddy simulations. Appl. Sci. Res. 57, 165–194.

Fleming, J.L., Simpson, R.L., Cowling, J.E., Devenport, W.J., 1993. An experimental study of wing–body junction and wake flow. Exp. Fluids 14, 366–378.

Fu, S., Launder, B.E., Tselepidakis, D.P., 1987a. Accommodating the effects of high strain rates in modelling the pressure–strain correlation. Report TFD/87/5 Mechanical Engineering Department, UMIST, Manchester.

Fu, S., Leschziner, M.A., Launder, B.E., 1987b. Modelling strongly swirling recirculating jet flow with Reynolds-stress transport closure. In: Proceedings of the Sixth Symposium on Turbulent Shear Flow.Toulouse, pp. 17.6.1–17.6.6.

Fu, S., Huang, P.G., Launder, B.E., Leschziner, M.A., 1988. A comparison of algebraic and differential second-moment closures for axisymmetric turbulent shear flows with and without swirl. ASME J. Fluids Eng. 110, 216–222.

Gatski, T.B., Speziale, C.G., 1993. On explicit algebraic stress models for complex turbulent flows. J. Fluid Mech. 254, 59–78.

Gerolymos, G.A., Vallet, I., 1996. Implicit computation of three-dimensional compressible Navier–Stokes equations using k–ε closure. AIAA J. 34, 1321–1330.

Gerolymos, G.A., Vallet, I., 1997. Near-wall Reynolds-stress three-dimensional transonic flow computation. AIAA J. 35, 228–236.

Gibson, M.M., Dafa'Alla, A.A., 1995. Two-equation model for turbulent wall flow. AIAA J. 33, 1514–1518.

Gibson, M.M., Launder, B.E., 1978. Ground effects on pressure fluctuations in the atmospheric boundary layer. J. Fluid Mech. 86, 491.

Gilbert, N., Kleiser, L., 1991. Turbulence model testing with the aid of direct numerical simulation results. In: Proceedings of the Eighth Symposium on Turbulent Shear Flows. Munich, pp. 26.1.1–26.1.6.

Girimaji, S.S., 1997. A Galilean invariant explicit algebraic Reynolds stress model for turbulent curved flows. Phys. Fluids 1067–1077.

Goldberg, U.C., 1994. Towards a pointwise turbulence model for wall-bounded and free shear flows. ASME J. Fluids Eng. 116, 72.

Haase, W., Brandsma, F., Elsholz, E., Leschziner, M.A., Schwamborn, D. (Eds.), 1993. EUROVAL—A European Initiative on Validation of CFD Codes—Results of the EC/BRITE-EURAM Project EUROVAL, 1990–1992, Notes on Numerical Fluid Mechanics, vol. 42, Vieweg, Brsunschweig.

Haase, W., Chaput, E., Elsholz, E., Leschziner, M.A., Müller, U.R. (Eds.), 1996. ECARP: European Computational Aerodynamics Research Project. II: Validation of CFD Codes and Assessment of Turbulent Models, Notes on Numerical Fluid Mechanics, vol. 58, Vieweg, Brsunschweig.

Haidinger, F.A., Friedrich, R., 1993. Computation of shock wave/boundary layer interactions using a two-equation model with compressibility corrections. Appl. Sci. Res. 51, 501–505.

Haidinger, F.A., Friedrich, R., 1995. Numerical simulation of strong shock/turbulent boundary layer interaction using a Reynolds stress model. Z. Flugwiss. Weltraumforschung 19, 10–18.

Hallbaeck, M., Groth, A., Johansson, A.V., 1991. Anisotropic dissipation rate—implications for Reynolds-stress models. In: Johansson, A.V., Alfredson, P.H. (Eds.), Advances in Turbulence. Springer, Berlin, pp. 414–421.

Hanjalić, K., 1994. Advanced turbulence closure models: a view of current status and future prospects. Int. J. Heat Fluid Flow 15, 178–203.

Hanjalić, K., Jakirlić, S., 1993. A model of stress dissipation in second moment closures. Appl. Sci. Res. 51, 513–518.

Hanjalić, K., Launder, B.E., 1972. A Reynolds stress model and its application to thin shear flows. J. Fluid Mech. 52, 609–638.

Hasan, R.G.M., McGuirk, J.J., Apsley, D.D., Leschziner, M.A., 2001. A turbulence model study of separated 3D jet/afterbody flow. Aeronaut. J. Paper 2760.

Hoffman, G.H., 1975. Improved form of low Reynolds-number k–ε turbulence model. Phys. Fluids 18, 309–312.

Huang, P.G., 1990. Modelling hypersonic boundary layers with second moment closure. CTR, University of Stanford, Ann. Res. Briefs, 1–13.

Huang, P.G., 1997. Validation of turbulence model—uncertainties and measures to reduce them. Proceedings of the ASME FED Summer Meeting, June 22–26.

Huang, P.G., Coakley, T.J., 1993. Modelling hypersonic flows with second-moment closure. In: So, R.M.C., Speziale, C.G., Launder, B.E. (Eds.), Near-Wall Turbulent Flows. Elsevier, Amsterdam, pp. 199–208.

Huang, P.G., Bradshaw, P., Coakley, T.J., 1994. Turbulence models for compressible boundary-layers. AIAA J. 32, 735–740.

Huang, P.G., Coleman, G.N., Bradshaw, P., 1995. Compressible turbulent channel flows—DNS results and modelling. J. Fluid Mech. 305, 185–218.

Ince, N.Z., Betts, P.L., Launder, B.E., 1994. Low Reynolds number modelling of turbulent buoyant flows. In: Henkes, R.A.W.M., Hoogendoorn, C.J. (Eds.), Proceedings of the EUROTHERM Seminar, vol. 22, Turbulent Natural Convection in Cavities, Delft, Editions européenes Thermique et Industrie, Paris, p. 76.

Jakirlić, S., 1997. Reynolds-spannungs-modellierung komplexer turbulenter Stroemungen. Ph.D. Thesis, University of Erlangen-Nuernberg.

Jakirlić, S., Hanjalić, K., 1995. A second-moment closure for non-equilibrium and separating high- and low-Re-number flows. In: Proceedings of the 10th Symposium on Turbulent Shear Flows.Pennsylvania State University, p. 23.25.

Jang, Y.-J., Leschziner, M.A., Abe, K., Temmerman, L., 2002. Investigation of anisotropy resolving turbulence models by reference to highly-resolved LES data for separated flow. Flow, Turb. Combust. 69, 161–203.

Johansson, M.C., Knoell, J., Taulbee, D.B., 2000. Nonlinear stress–strain model accounting for dissipation anisotropies. AIAA J. 38, 2187–2189.

Jones, W.P., Launder, B.E., 1972. The prediction of laminarization with a two-equation model of turbulence. Int. J. Heat Mass Transfer 15, 301–314.

Jongen, T., Gatski, T.B., 1998. General explicit algebraic stress relations and best approximation for three-dimensional flows. Int. J. Eng. Sci. 36, 739–763.

Kalitzin, G., Gould, A.R.B., Benton, J.J., 1996. Application of two-equation turbulence models in aircraft design. AIAA Paper 96-0327.

Kassinos, S.C., Langer, C.A., Haire, S.L., Reynolds, W.C., 2000. Structure-based modelling for wall-bounded flows. Int. J. Heat Fluid Flow 21, 599–605.

Kawamura, H., Kawashima, N., 1994. A proposal for a k–ε model with relevance to the near-wall turbulence. Paper IP.1, Proceedings of the International Symposium on Turbulence, Heat and Mass Transfer, Lisbon.

Lam, C.K.G., Bremhorst, K., 1981. A modified form of the k–ε model for predicting wall turbulence. J. Fluids Eng. 103, 456–460.

Launder, B.E., Reynolds, W.C., 1983. Asymptotic near-wall stress dissipation rates in turbulent flow. Phys. Fluids 26, 1157.

Launder, B.E., Sharma, B.I., 1974. Application of the energy-dissipation model of turbulence to the calculation of flow near a spinning disc. Lett. Heat Mass Transfer 1, 131.

Launder, B.E., Shima, N., 1989. Second-moment closure for the near-wall sublayer. AIAA J. 27, 1319–1325.

Launder, B.E., Tselepidakis, D.P., 1993. Contribution to the modelling of near-wall turbulence. In: Durst, F., et al. (Eds.), Turbulent Shear Flows, vol. 8. Springer, Berlin, p. 81.

Launder, B.E., Reece, G.J., Rodi, W., 1975. Progress in the development of Reynolds-stress turbulence closure. J. Fluid Mech. 68, 537–566.

Launder, B.E., Priddin, C.H., Sharma, B., 1977. The calculation of turbulent boundary layers on curved and spinning surfaces. ASME J. Fluids Eng. 98, 753.

Leschziner, M.A., Dimitriadis, K.P., Page, G., 1993. Computational modelling of shock wave/boundary layer interaction with a cell-vertex scheme and transport models of turbulence. Aeronaut. J. 97, 43–61.

Leschziner, M.A., Batten, P., Loyau, H., 2000a. Modelling shock-affected near-wall flows with anisotropy-resolving turbulence closures. Int. J. Heat Fluid Flow 21, 239–251.

Leschziner, M.A., Loyau, H., Apsley, D.D., 2000b. Prediction of shock/boundary-layer interaction with non-linear eddy-viscosity models. CDROM Proceedings of the European Congress on Computational Methods in Applied Sciences and Engineering, CDR Proceedings ECCOMAS 2000, Barcelona.

Leschziner, M.A., Batten, P., Craft, T.J., 2001. Reynolds-stress modelling of afterbody flows. Aeronaut. J. 105, 297–306.

Lien, F.S., Durbin, P.A., 1996. Non-linear k–v^2 modelling with application to high-lift. In: Proceedings of the Summer Program Centre for Turbulence Research.Stanford University, pp. 5–22.

Lien, F.S., Leschziner, M.A., 1993. A pressure–velocity solution strategy for compressible flow and its application to shock/boundary-layer interaction using second-moment turbulence closure. J. Fluids Eng. 115, 717–725.

Lien, F.S., Leschziner, M.A., 1994. Modelling the flow in a transition duct with a non-orthogonal FV procedure and low-Re turbulence-transport models. Proceedings of the ASME FED Summer Meeting, Symposium on Advances in Computational Methods in Fluid Dynamics, pp. 93–106.

Lien, F.S., Leschziner, M.A., 1995. Modelling 2D separation from high-lift aerofoil with non-linear eddy-viscosity model and second-moment closure. Aeronaut. J. 99, 125–144.

Lien, F.S., Leschziner, M.A., 1997. Computational modelling of separated flow around streamlined body at high incidence. Aeronaut. J. 101, 269–275.

Lien, F.S., Chen, W.L., Leschziner, M.A., 1996. Low-Reynolds-number eddy-viscosity modelling based on non-linear stress–strain/vorticity relations. In: Rodi, W., Bergeles, G. (Eds.), Engineering Turbulence Modelling and Measurements, vol. 3. Elsevier, Amsterdam, pp. 91–100.

Liou, W.W., Huang, G., Shih, T.-H., 2000. Turbulence model assessment for shock wave/turbulent boundary-layer interaction in transonic and supersonic flow. Comput. Fluids 29, 275–299.

Loyau, H., Batten, P., Leschziner, M.A., 1998. Modeling shock/boundary-layer interaction with nonlinear eddy-viscosity closures. Flow, Turb. Combust. 60, 257–282.

Lumley, J.L., 1978. Computational modelling of turbulent flows. Adv. Appl. Mech. 18, 123–176.

Marvin, J.G., Huang, P.G., 1996. Turbulence modelling—progress and future outlook. In: Proceedings of the 15th Conference on Numerical Methods in Fluid Dynamics.Monterey, California.

Meier, H.U., Kreplin, H.P., Landhauser, A., Baumgarten D., 1984. Mean velocity distribution in 3D boundary layers developing on a 1:6 prolate spheroid with artificial transition. DFVLR Report IB 222-84 A11.

Menter, F.R., 1992a. Influence of freestream values on k–ω turbulence model predictions. AIAA J. 30, 1657–1659.

Menter, F.R., 1992b. Performance of popular turbulence models for attached and separated adverse pressure gradient flows. AIAA J. 30, 2066–2072.

Menter, F.R., 1994. Two equation eddy viscosity turbulence models for engineering applications. AIAA J. 32, 1598–1605.

Menter, F.R., 1997. Eddy viscosity transport equations and their relation to the k–ε model. ASME J. Fluids Eng. 119, 876–884.

Morrison, J.H., Gatski, T.B., Sommer, T.P., So, R.M.C., 1993. Evaluation of a near-wall turbulent closure model in predicting compressible ramp flows. In: So, R.M.C., Speziale, C.G., Launder, B.E. (Eds.), Near-Wall Turbulent Flows. Elsevier, Amsterdam, pp. 239–250.

Myong, H.K., Kasagi, N., 1990. A new approach to the improvement of k–ε turbulence model for wall bounded shear flows. JSME Int. J. II 33, 63–72.

Nagano, Y., Hishida, M., 1987. Improved form of the k–ε model for turbulent shear flows. Trans. of ASME. 109, 156.

Oberlack, M., 1997. Non-isotropic dissipation in non-homogeneous turbulence. J. Fluid Mech. 350, 351–374.

Obi, S., Aoki, K., Masuda, S., 1993. Experimental and computational study of turbulent separated flow in an asymmetric diffuser. In: Proceedings of the Ninth Symposium on Turbulent Shear Flows.Kyoto, pp. 305–307.

Orszag, S.A., Yakhot, V., Flannery, W.S., Boysan, F., Choudhury, D., Maruzewski, J., Patel, B., 1993. Renormalisation group modelling and turbulence simulations. In: So, R.M.C., Speziale, C.G., Launder, B.E. (Eds.), Near-Wall Turbulent Flows. Elsevier, Amsterdam, pp. 1031–1046.

Parneix, S., Durbin, P.A., Behnia, M., 1998. Computation of 3-D turbulent boundary layers using the V2F model. Flow, Turb. Combust. 60, 19–46.
Pfunderer, D.G., Eifert, C., Janicka, J., 1997. Nonlinear second moment closure consistent with shear and strain flows. AIAA J. 35, 825–831.
Piccin, O., Cassoudesalle, D., 1987. Etude dans la soufflerie F1 des profils AS239 et AS240. ONERA Technical Report, PV 73/1685 AYG.
Pope, S.B., 1975. A more general effective-viscosity hypothesis. J. Fluid Mech. 72, 331–340.
Putnam, L.E., Mercer, C.E., 1986. Pitot-pressure measurements in flow fields behind a rectangular nozzle with exhaust jet for free-stream Mach numbers of 0, 0.6 and 1.2. NASA TM 88990.
Robinson, D.F., Hasan, H.A., 1998. Further developments of the k–ζ (enstrophy) turbulence closure model. AIAA J. 36, 1825–1833.
Rodi, W., 1976. A new algebraic relation for calculating the Reynolds stresses. Z. Angew. Math. Mech. 56, 219–221.
Rodi, W., 1979. Influence of buoyancy and rotation on equations for the turbulent length scale. In: Proceedings of the Second Symposium on Turbulent Shear Flows.London, pp. 10.37–10.42.
Rodi, W., Scheuerer, G., 1983. Calculation of curved shear layers with two-equation turbulence models. Phys. Fluids 26, 1422.
Rotta, J.C., 1951. Statistische Theory nichhomogener Turbulenz. Z. Physik 129, 547.
Rubinstein, R., Barton, J.M., 1990. Non-linear Reynolds stress models and the renormalisation group. Phys. Fluids A 2, 1472–1476.
Rumsey, C.L., Gatsky, T.L., Morrison, J.H., 1999. Turbulence model predictions of extra strain rate effects in strongly curved flows. AIAA Paper 99–157.
Rung, T., Fu, S., Thiele, F., 1999a. On the realisability of non-linear stress–strain relation for Reynolds-stress closures. Flow, Turb. Combust. 60, 333–359.
Rung, T., Luebke, H., Franke, M., Xue, L., Thiele, F., Fu, S., 1999b. Assessment of explicit algebraic stress models in transonic flows. In: Rodi, W., Laurence, D. (Eds.), Engineering Turbulence Modelling and Experiments, vol. 4. Elsevier, Amsterdam, pp. 659–668.
Saffman, P.G., 1977. Results of a two-equation model for turbulent and development of a relaxation stress model for application to straining and rotating flows. In: Murthy, S. (Ed.), Proceedings of the Project SQUID Workshop on Turbulence in Internal Flows. Hemisphere Press, Washington, DC, pp. 191–231.
Sarkar, S., 1992. The pressure–dilatation correlation in compressible flows. Phys. Fluid 282, 163–186.
Sarkar, S., Erlebacher, G., Hussaini, M.Y., Kreiss, H.O., 1991. The analysis and modelling of dilatational terms in compressible turbulence. J. Fluid Mech. 227, 473–493.
Schiestel, R., 1987. Multiple time scale modelling of turbulent flows in one point closures. Phys. Fluids. 30, 722.
Schmitt, V., Charpin, F., 1979. Pressure distributions on the ONERA M6 wing at transonic Mach numbers. AGARD AR-138.
Shih, T.H., Lumley, J.L., 1985. Modelling of pressure correlation terms in Reynolds-stress and scalar-flux equations. Report FDA-85-3, Sibley School of Mechanics and Aerospace Engineering, Cornell University.
Shih, T.-h., Zhu, J., Lumley, J.L., 1993. A realisable Reynolds stress algebraic equation model. NASA TM105993.
Shima, N., 1988. A Reynolds-stress model for near-wall and low-Reynolds-number regions. ASME J. Fluids Eng. 110, 38–44.
Simpson, R.L., Long, C.H., Byun, G., 2002. Study of vortical separation from an axisymmetric hill. Int. J. Heat Fluid Flow 23, 582–591.
So, R.M.C., Lai, Y.G., Zhang, H.S., Hwang, B.C., 1991a. Second-order near-wall turbulence closures: a review. AIAA J. 29, 1819–1835.
So, R.M.C., Zhang, H.S., Speziale, C.G., 1991b. Near-wall modelling of the dissipation rate equation. AIAA J. 29, 2069–2076.
Spalart P.R., Allmaras, S.R., 1992. A one-equation turbulence model for aerodynamic flows. AIAA Paper 92-0439.
Spalart, P.R., Jou, W.-J., Strelets, M., Allmaras, S.R., 1997. Comments on the feasibility of LES for wings and on the hybrid RANS/LES approach. Advances in DNS/LES, First AFOSR International Conference on DNS/LES, Greden Press.
Speziale, C.G., 1987. On nonlinear K-l and K-ε models of turbulence. J. Fluid Mech. 178, 459–475.
Speziale, C.G., Sarkar, S., Gatski, T.B., 1991. Modelling the pressure–strain correlation of turbulence: an invariant dynamical systems approach. J. Fluid Mech. 227, 245.
Speziale, C.G., Abid, R., Anderson, E.C., 1992. Critical evaluation of two-equation models for near-wall turbulence. AIAA J. 30, 324–331.
Srinivasan, G.R., Ekaterinaris, J.A., McCroskey, W.J., 1993. Dynamic stall of an oscillating wing, part 1: evaluation of turbulence models. AIAA Paper 93-3403.

Taulbee, D.B., Sonnenmeier, J.R., Wall, K.M., 1993. Application of a new non-linear stress–strain model to axisymmetric turbulent swirling flows. In: Rodi, W., Martelli, F. (Eds.), Engineering Turbulence Modelling and Experiments, vol. 2. Elsevier, Amsterdam, pp. 103–112.

Temmerman, L., Leschziner, M., Mellen, C., Froehlich, J., 2003. Investigation of subgrid-scale models and wall-function approximations in Large Eddy Simulation of separated flow in a channel with streamwise periodic constrictions. Int. J. Heat Fluid Flow 24, 157–180.

Temmerman, L., Chen, W., Leschziner, M.A., 2004. A comparative study of separation from a three-dimensional hill using LES and second-moment-closure RANS modeling, fourth European Congress on Computational Methods in Applied Sciences and Engineering, ECCOMAS 2004, Jyvaskyla, Finnland (CDR proceedings).

Vandromme, D., Haminh, H., 1985. Physical analysis for turbulent boundary-layer/shock-wave interactions using second-moment closure predictions. In: Delery, J. (Ed.), Turbulent Shear-Layer/Shock-Wave Interactions. Springer, Berlin, pp. 127–136.

Wallin, S., Johansson, A.V., 1997. A new explicit algebraic Reynolds stress turbulence model for 3D flows. In: Durst, F. et al. (Eds.), Proceedings of the 11th Symposium on Turbulent Shear Flows. Grenoble, pp. 13.13–13.17.

Wallin, S., Johansson, A.V., 2000. An explicit algebraic Reynolds stress model for incompressible and compressible turbulent flows. J. Fluid Mech. 403, 89–132.

Wallin, S., Johansson, A.V., 2001. Modelling of streamline curvature effects on turbulence in explicit algebraic Reynolds stress turbulence models. In: Proceedings of the Second International Symposium on Turbulence and Shear Flow Phenomena.Stockholm, pp. 223–228.

Wang, C., Jang, Y.J., Leschziner, M.A., 2004. Modelling two- and three-dimensional separation from curved surfaces with anisotropy-resolving turbulence closures. Int. J Heat and Fluid Flow 25, 499–512.

Wilcox, D.C., 1988a. Multi-scale model for turbulent flows. AIAA J. 26, 1311–1320.

Wilcox, D.C., 1988b. Reassessment of the scale-determining equation for advanced turbulence models. AIAA J. 26, 1299–1310.

Wilcox, D.C., 1993. Turbulence Modelling for CFD. DCW Industries, La Canada, California.

Wilcox, D.C., 1994. Simulation transition with a two-equation turbulence model. AIAA J. 32, 247–255.

Wilcox, D.C., Rubesin, M.W., 1980. Progress in turbulence modelling for complex flow field including effects of compressibility. NASA TP1517.

Xu, X.-H., Speziale, C.G., 1996. Explicit algebraic stress model of turbulence with anisotropic dissipation. AIAA J. 34, 2186–2189.

Yap, C.R., 1987. Turbulent heat and momentum transfer in recirculating and impinging flows. Ph.D. Thesis, University of Manchester.

Yoshizawa, A., 1987. Statistical analysis of the derivation of the Reynolds stress from its eddy-viscosity representation. Phys. Fluids 27, 1377–1387.

Younis, B.A., Gatski, T.B., Speziale, C.G., 2000. Towards a rational model for the triple velocity correlations of turbulence. Proc. R. Soc. London A 456, 909–920.

Zeman, O., 1990. Dilatation dissipation: the concept and application in modelling compressible mixing layers. Phys. Fluids 2, 178–188.

Zeman, O., 1993. New model for super/hypersonic turbulent boundary layers. AIAA Paper 93-0897.

Zhou, G., Davidson, L., Olsson, E., 1995. Turbulent transonic airfoil flow simulation using a pressure-based algorithm. AIAA J. 33, 42–47.